Application of computational modelling to the study of complex biological events related to fertility

Nicola Bernabò PhD DMV

Faculty of Bioscience and Technology for Food, Agriculture and Environment
University of Teramo

Infertility is “a disease of the reproductive system defined by the failure to achieve a clinical pregnancy after 12 months or more of regular unprotected sexual intercourse.”… (WHO-ICMART glossary).

SPECIAL CONTRIBUTION

International Committee for Monitoring Assisted Reproductive Technology (ICMART) and the World Health Organization (WHO) revised glossary of ART terminology, 2009*

F. Zegers-Hochschild,[a] G. D. Adamson,[b] J. de Mouzon,[c] O. Ishihara,[d] R. Mansour,[e] K. Nygren,[f] E. Sullivan,[g] and S. Vanderpoel,[h] for ICMART and WHO

[a] Unit of Reproductive Medicine, Clinicas las Condes, Santiago, Chile; [b] Fertility Physicians of Northern California, Palo Alto and San Jose, California; [c] INSERM U822, Hôpital de Bicêtre, Le Kremlin Bicêtre Cedex, Paris, France; [d] Saitama Medical University Hospital, Moroyama, Saitana, Japan; [e] Cairo, Egypt; [f] IVF Unit, Sophiahemmet Hospital, Stockholm, Sweden; [g] Perinatal and Reproductive Epidemiology and Research Unit, School of Women's and Children's Health, University of New South Wales, Sydney, Australia; and [h] Department of Reproductive Health and Research and the Special Program of Research, Development, and Research Training in Human Reproduction, World Health Organization, Geneva, Switzerland

Objective: Many definitions used in medically assisted reproduction (MAR) vary in different settings, making it difficult to standardize and compare procedures in different countries and regions. With the expansion of infertility interventions worldwide, including lower resource settings, the importance and value of a common nomenclature is critical. The objective is to develop an internationally accepted and continually updated set of definitions, which would be utilized to standardize and harmonize international data collection, and to assist in monitoring the availability, efficacy, and safety of assisted reproductive technology (ART) being practiced worldwide.
Method: Seventy-two clinicians, basic scientists, epidemiologists and social scientists gathered together at the World Health Organization headquarters in Geneva, Switzerland, in December 2008. Several months before, three working groups were established asresponsible for terminology in three specific areas: clinical conditions and procedures, laboratory procedures, and outcome measures. Each group reviewed the existing International Committee for Monitoring Assisted Reproductive Technology glossary, made recommendations for revisions and introduced new terms to be considered for glossary expansion.
Result(s): A consensus was reached on 87 terms, expanding the original glossary by 34 terms, which included definitions for numerous clinical and laboratory procedures. Special emphasis was placed in describing outcome measures, such as cumulative delivery rates and other markers of safety and efficacy in ART.
Conclusion(s): Standardized terminology should assist in analysis of worldwide trends in MAR interventions and in the comparison of ART outcomes across countries and regions. This glossary will contribute to a more standardized communication among professionals responsible for ART practice, as well as those responsible for national, regional, and international registries. (Fertil Steril® 2009;92:1520–4. ©2009 World Health Organization. All rights reserved. Published with permission.)

The need for standard definitions is critical for benchmarking the outcomes of assisted reproductive technology (ART) procedures, at both national and international levels. Increase in the use of ART treatment worldwide and the continuing discussions, controversies, and debates over measures of efficacy and safety have generated both scientific and public interest (1–4). Definitions used in medically assisted reproduction within different countries are frequently the result of adaptations to particular medical, cultural, and religious settings. However, when undertaking international data collection, standardization is necessary so that monitoring of efficacy, safety, and quality of procedures and multinational research can be undertaken.

The International Committee for Monitoring Assisted Reproductive Technology (ICMART), an entity responsible for the collection and dissemination of worldwide data on ART, published the first glossary of ART terminology in 2006 (5, 6). That particular glossary resulted from discussions by participants at an international meeting on “Medical, Ethical, and Social Aspects of Assisted Reproduction” organized by the World Health Organization (WHO) in 2001 (7).

Received September 9, 2009; revised and accepted September 9, 2009.
F.Z.-H. has nothing to disclose. G.D.A. has nothing to disclose. J.d.M. has nothing to disclose. O.I. has nothing to disclose. R.M. has nothing to disclose. K.N. has nothing to disclose. E.S. has nothing to disclose. S.V. has nothing to disclose.
The International Committee for Monitoring Assisted Reproductive Technology receives funding from the American Society for Reproductive Medicine, the Society for Assisted Reproductive Technology, the European Society for Human Reproduction and Embryology, the Fertility Society of Australia, the Latin American Network of Assisted Reproduction, the Japan Fertility Society, and the Middle East Fertility Society.
This glossary is simultaneously published in *Human Reproduction* (Vol. 24, Iss. 11).
Reprint requests: F. Zegers-Hochschild, Unit of Reproductive Medicine, Clinica las Condes, Lo Fontecilla, 441, Santiago, Chile (FAX: 56-2-6108167; E-mail: fzegers@clc.cl).

0015-0282/09/$36.00

doi:10.1016/j.fertnstert.2009.09.009

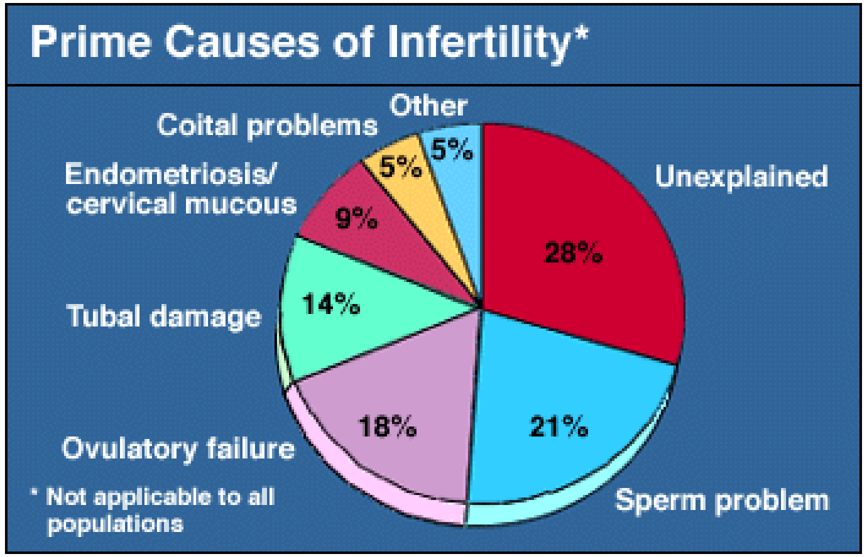

Prime causes of infertility. Causes of infertility in the U.S. Credits: Serono Laboratories

Fertilization: the biological context

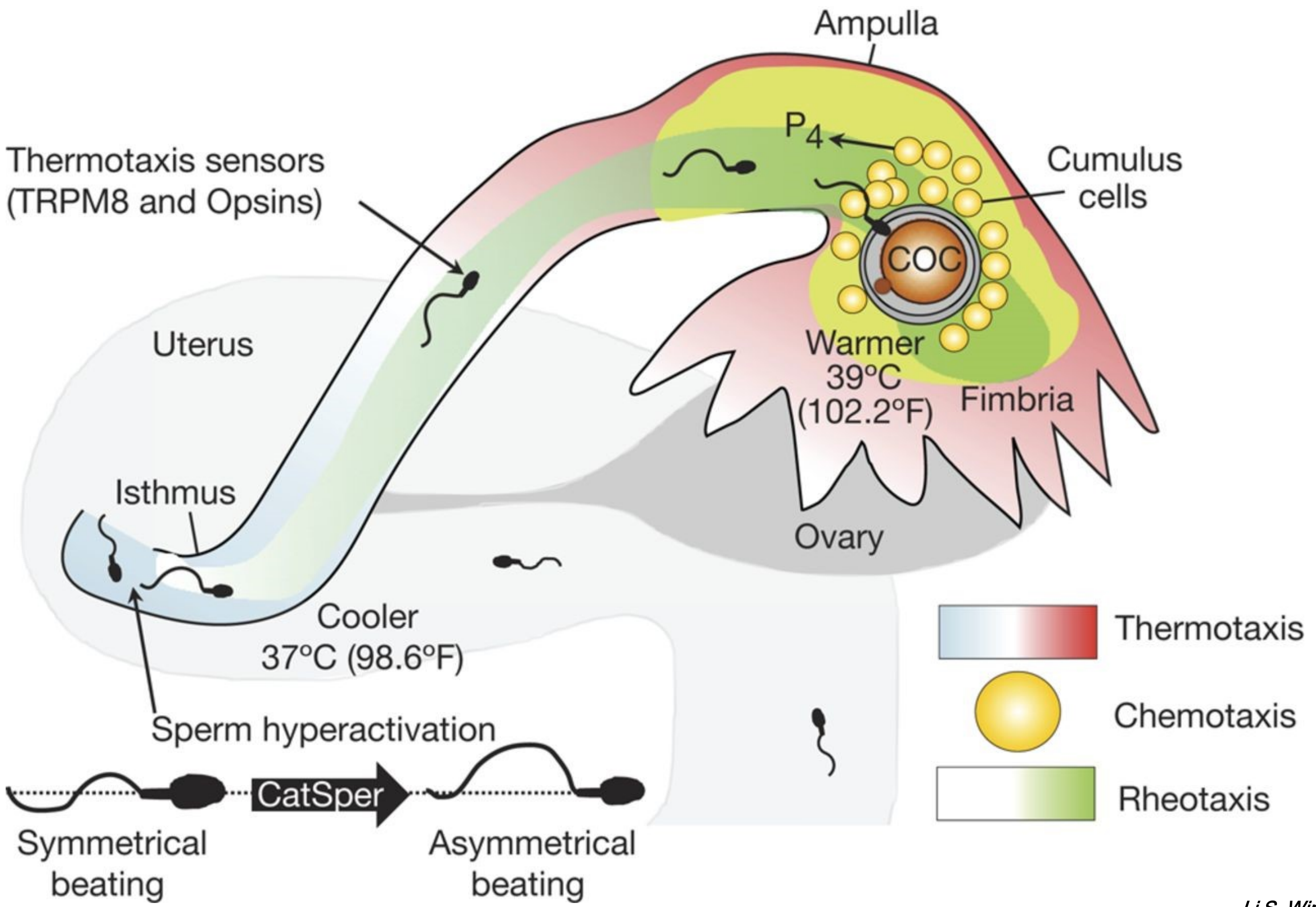

Li S, Winuthayanon W.. J Endocrinol. 2017 Jan;232(1):R1-R26

More in depth: Biological complexity

Complexity: non-linearity of interactions

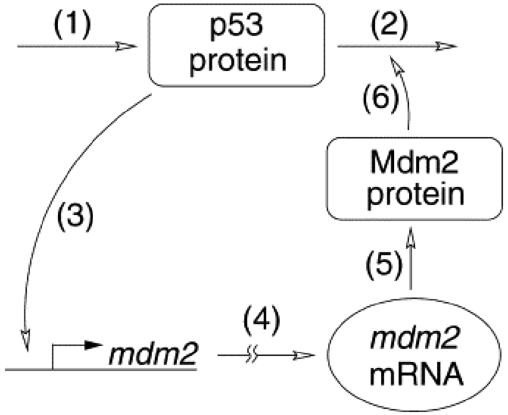

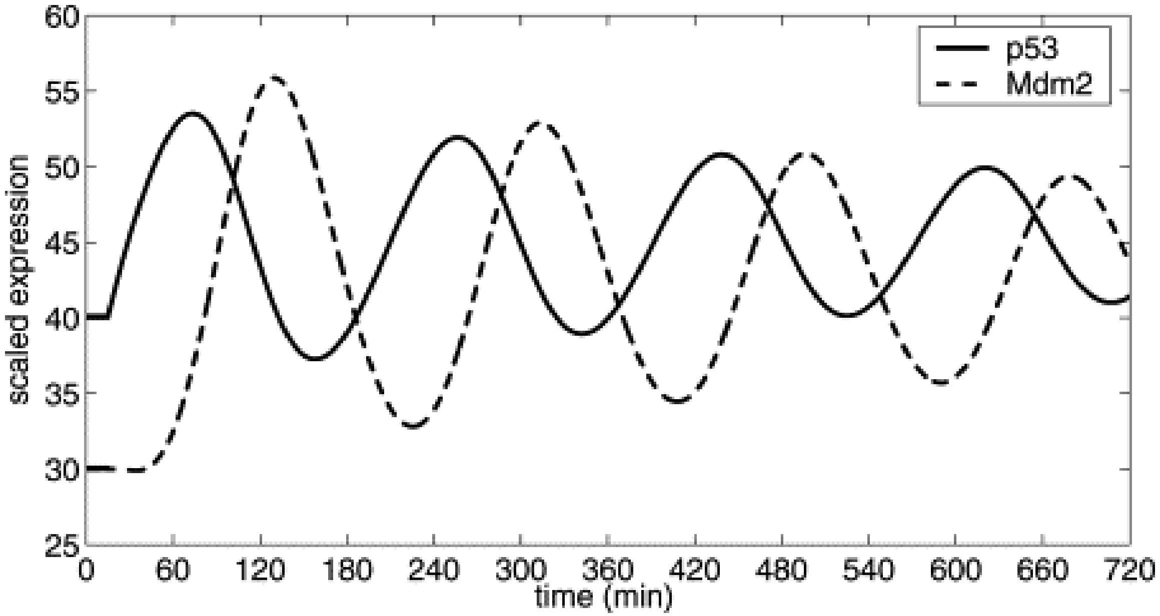

Complexity: unpredictability

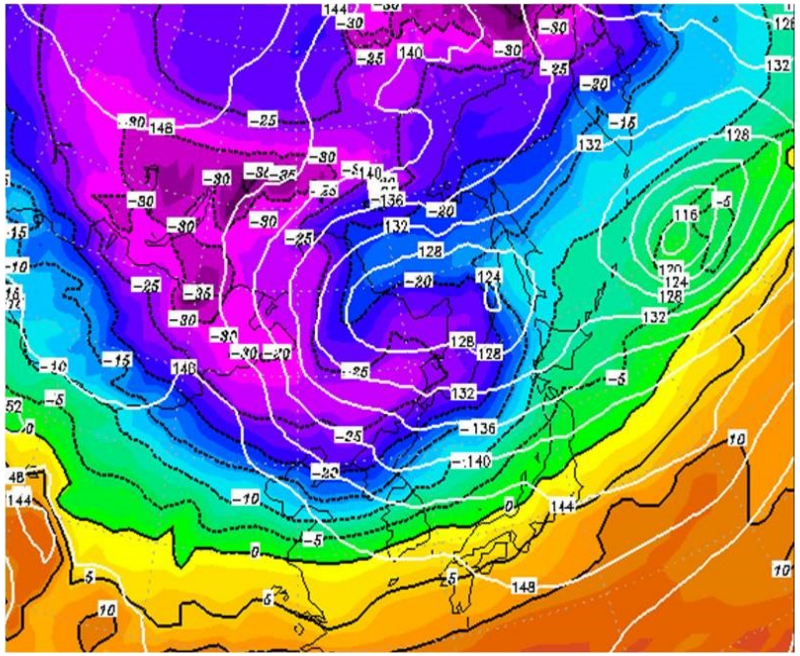

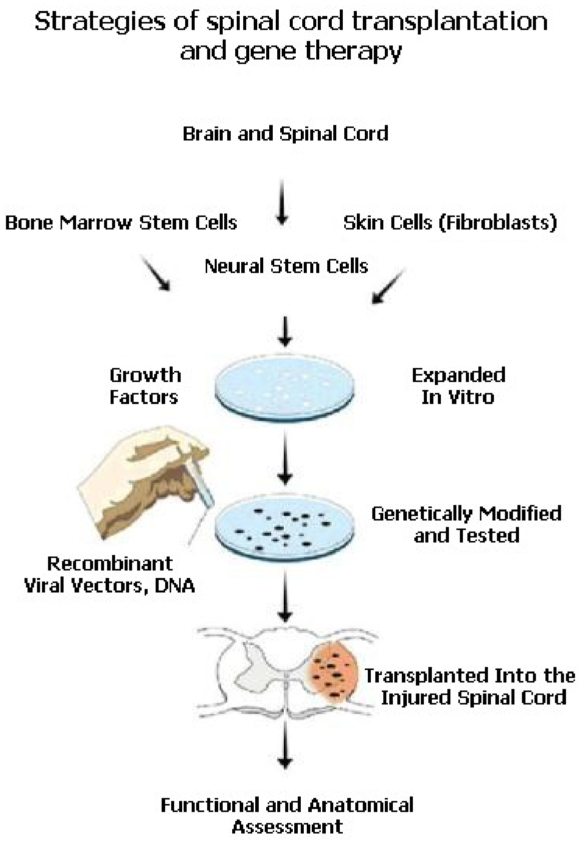

Complexity: the Butterfly effect

Complexity: the Emergence of proprieties

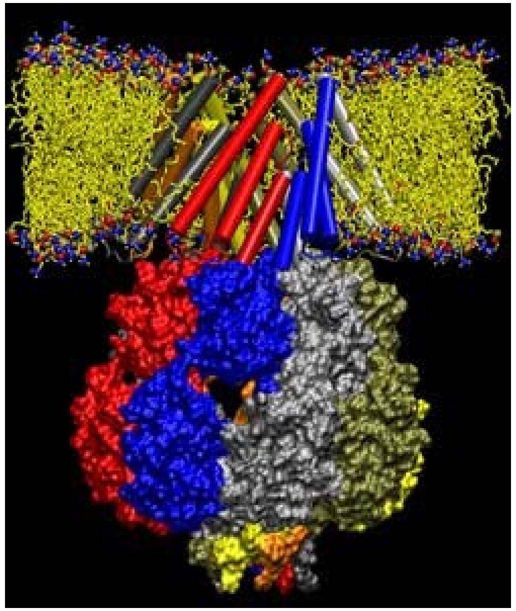 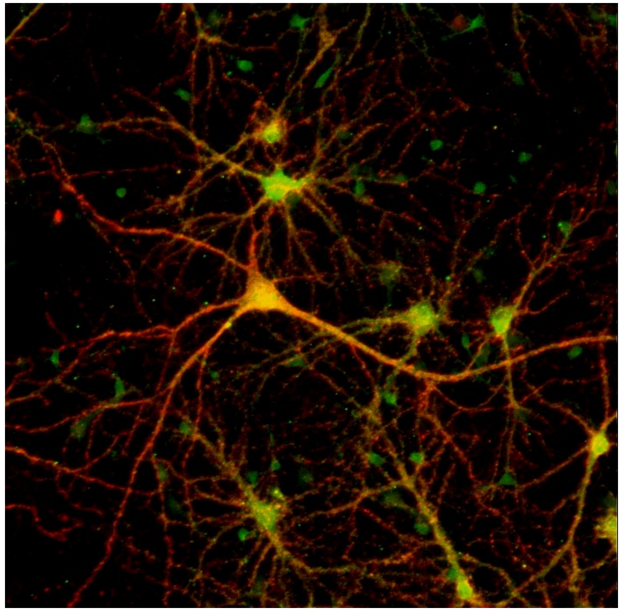 

The whole is more (different) than the sum of the individual components

Human Genome Project

Begun formally in 1990, the U.S. Human Genome Project was a 13-year effort coordinated by the U.S. Department of Energy and the National Institutes of Health. The project originally was planned to last 15 years, but rapid technological advances accelerated the completion date to 2003. Project goals

- *identify* all the approximately 20,000-25,000 genes in human DNA,
- *determine* the sequences of the 3 billion chemical base pairs that make up human DNA,
- *store* this information in databases,
- *improve* tools for data analysis,
- *transfer* related technologies to the private sector, and
- *address* the ethical, legal, and social issues (ELSI) that may arise from the project.

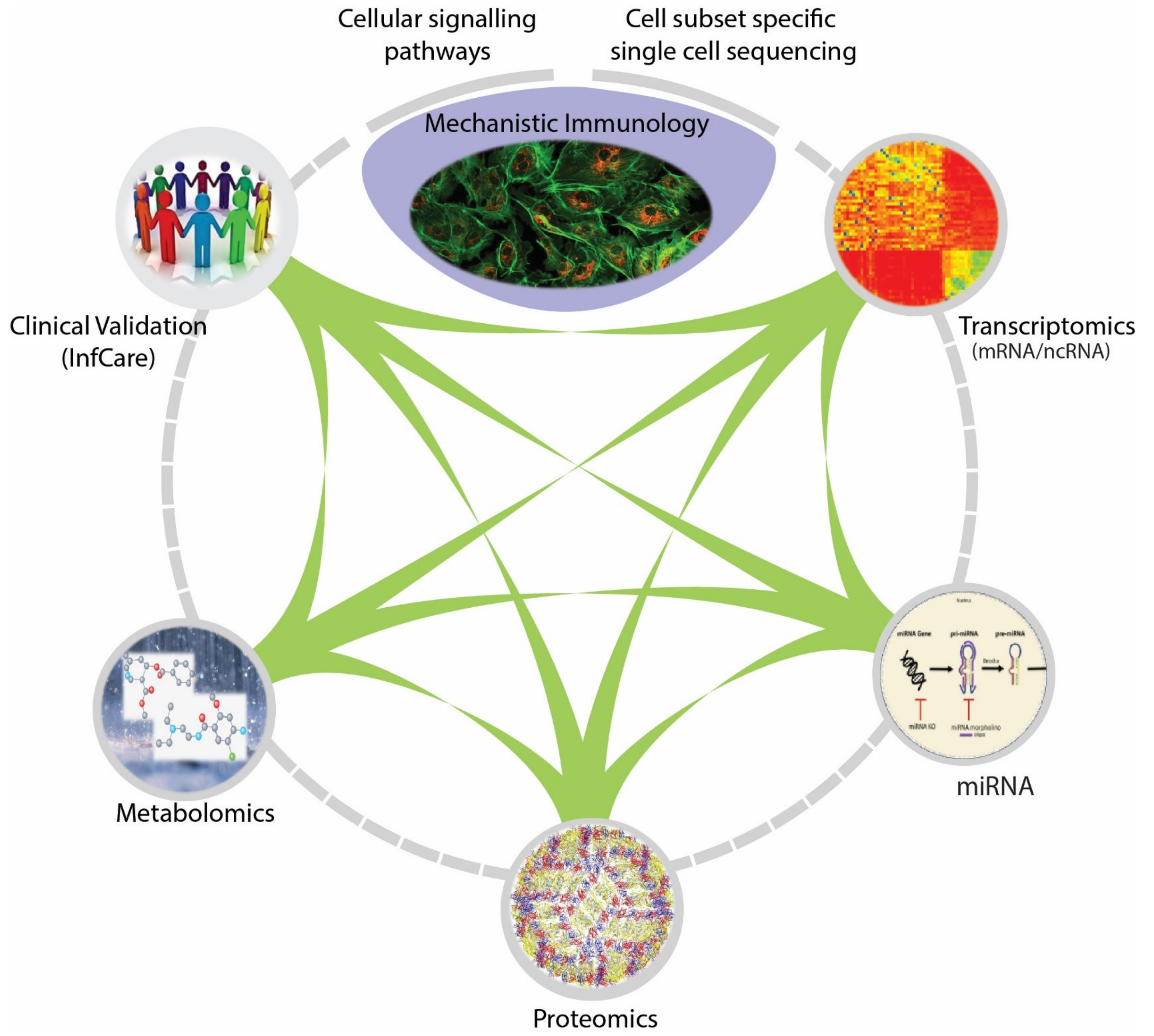

https://ki.se/en/labmed/team-multi-omics-research


N
ms
pm

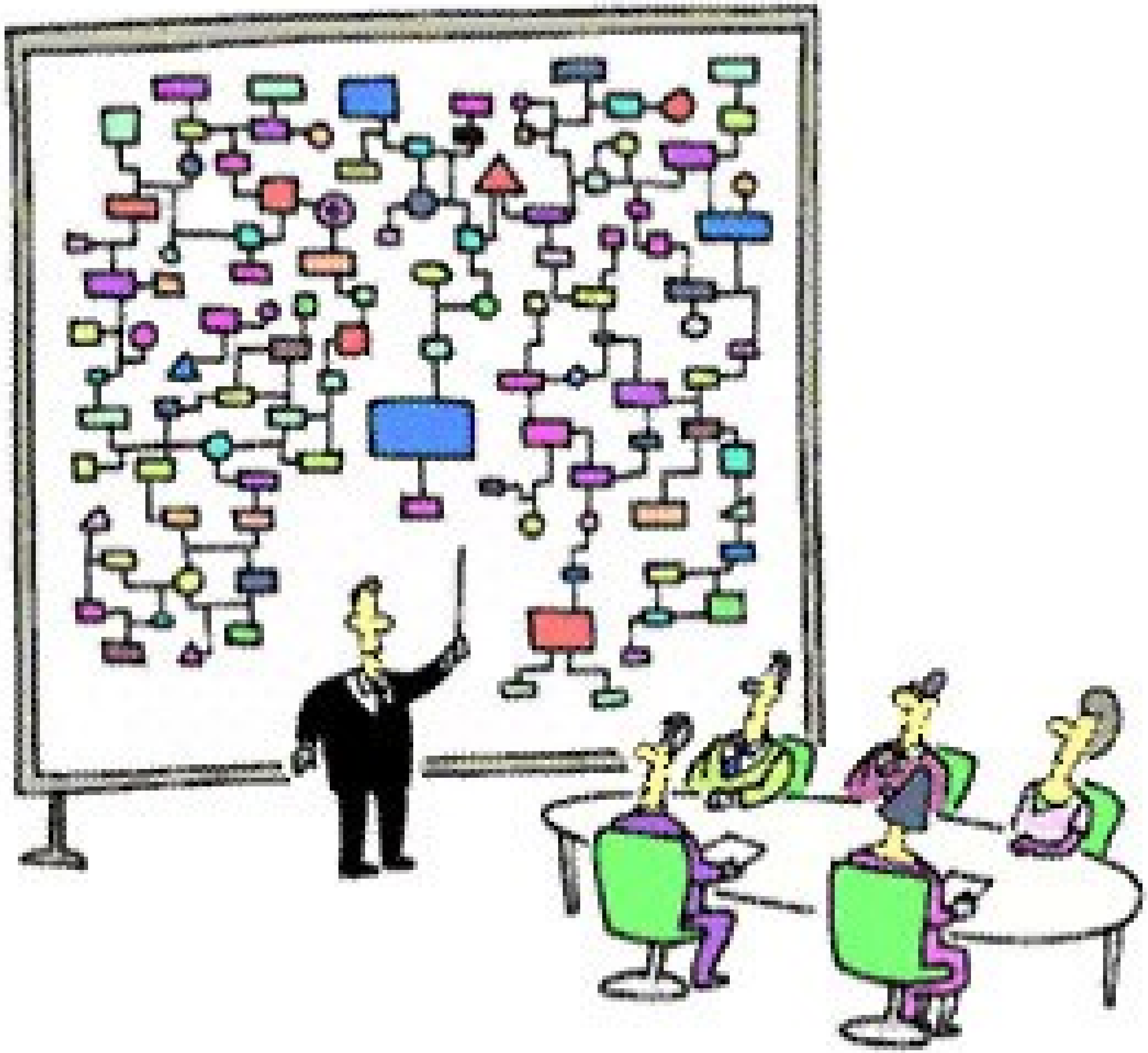

"And that's why we need a computer."

We need a model!

What is a model?

What kind of model we need?

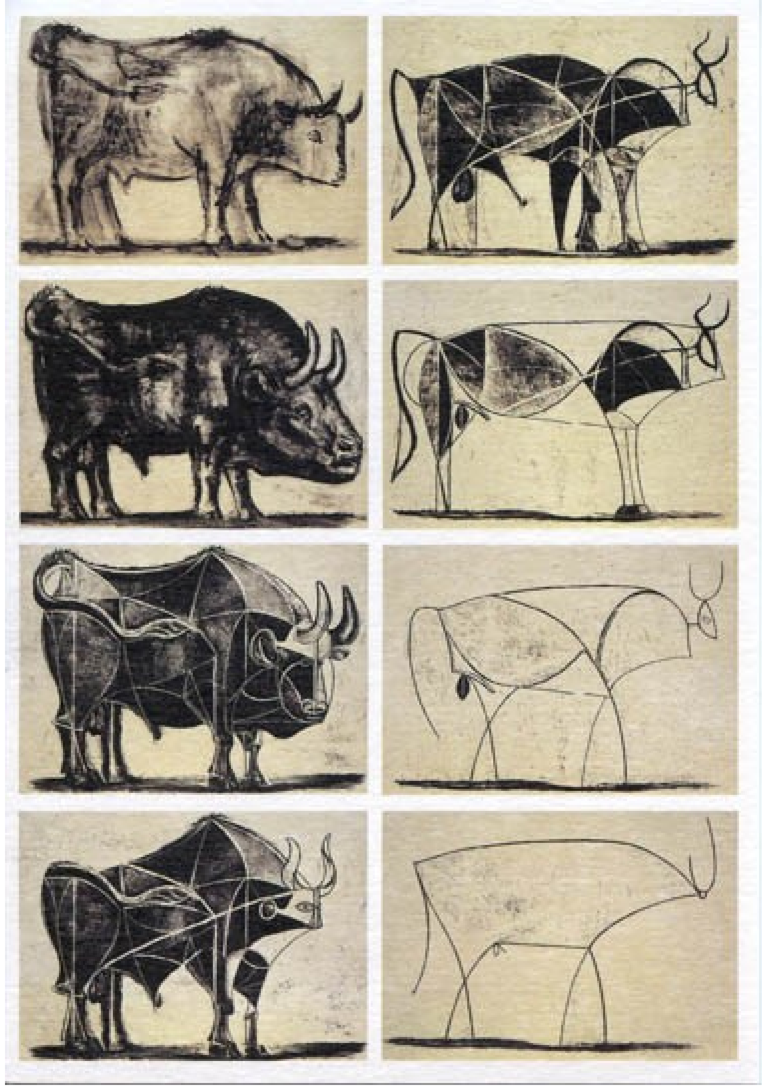

Numerical models

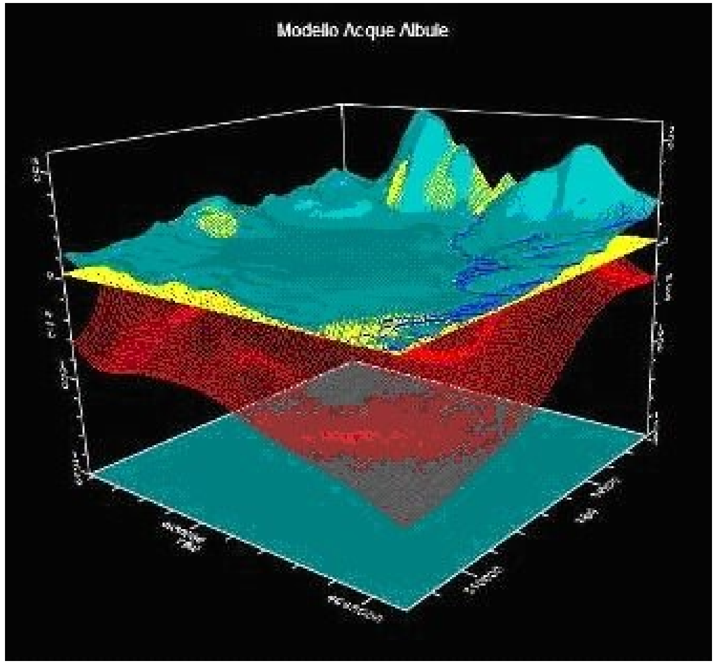

Networks as model

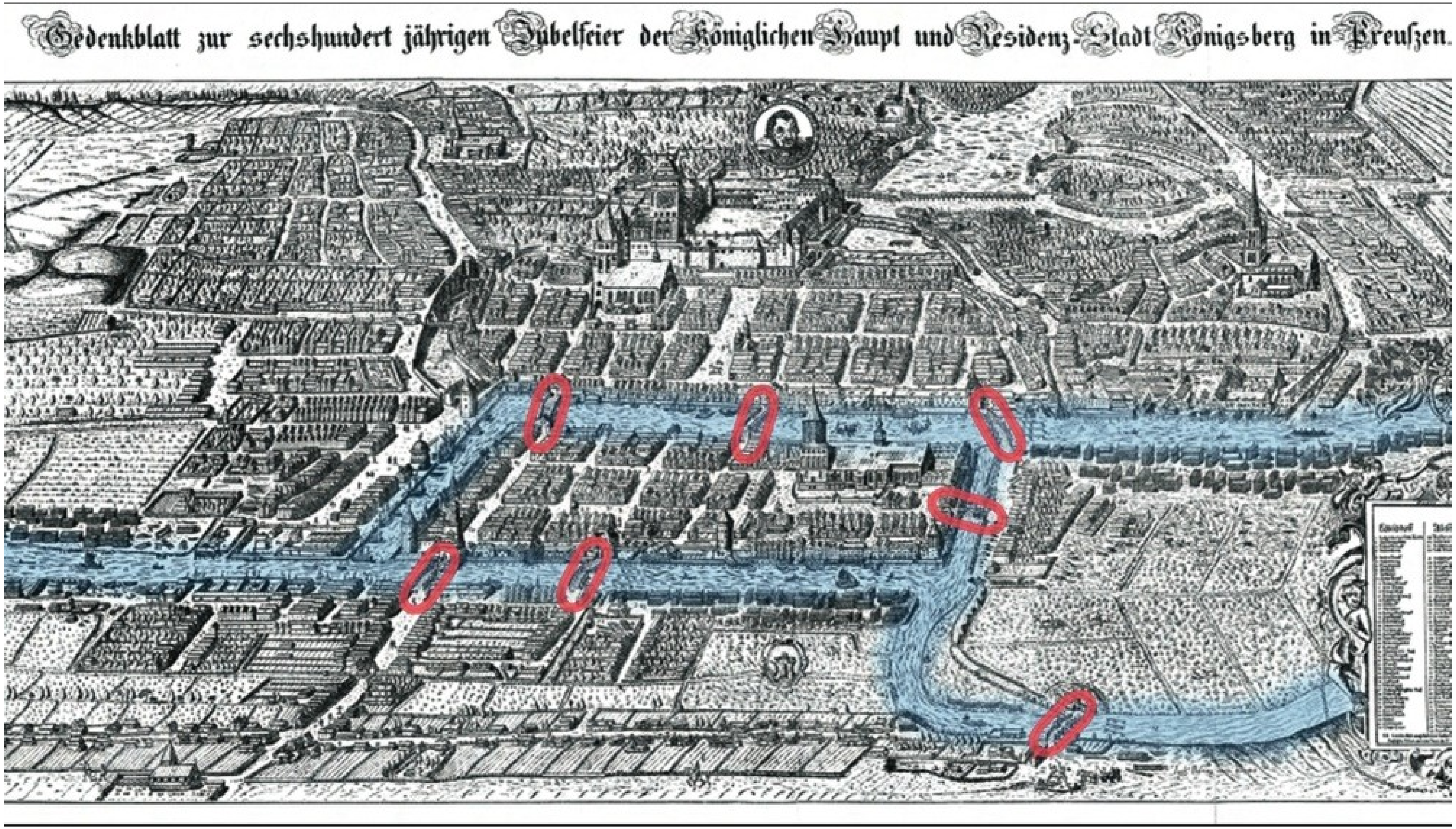

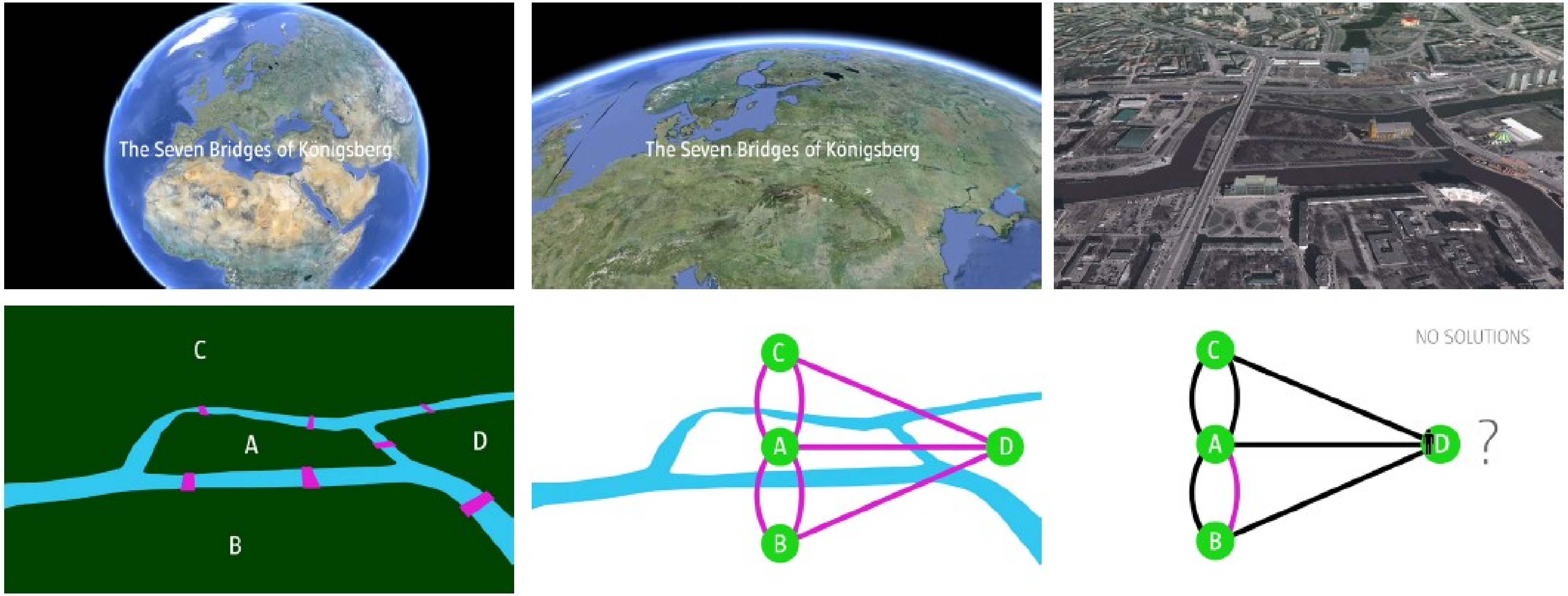

Image 2.1

The bridges of Königsberg.

From the contemporary map of Königsberg (now Kaliningrad, Russia) to Euler's graph. The graph constructed by Euler consists of four nodes (A, B, C, D), each corresponding to a patch of land, and seven links, each corresponding to a bridge. Euler showed in 1736 that there is no continuous path that would cross seven the bridges while never crossing the same bridge twice. The people of Königsberg agreed with him, gave up their fruitless search and in 1875 they built a new bridge between B and C, increasing the number of links of these two nodes to four. Now only one node was left with an odd number of links and it became rather straightforward to find the desired path.

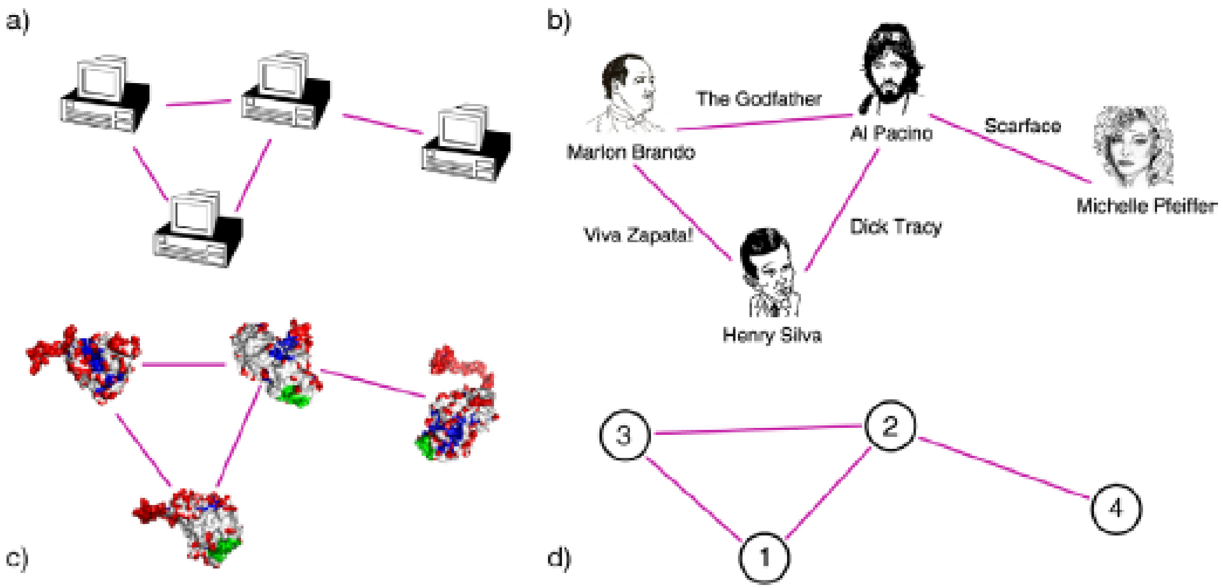

Image 2.3

Real systems of quite different nature can have the same network representation.

In the figure we show a small subset of (a) the *Internet*, where routers (specialized computers) are connected to each other; (b) the *Hollywood actor network*, where two actors are connected if they played in the same movie; (c) a *protein-protein interaction network*, where two proteins are connected if there is experimental evidence that they can bind to each other in the cell. While the nature of the nodes and the links differs widely, each network has the same graph representation, consisting of $N = 4$ nodes and $L = 4$ links, shown in (d).

The node

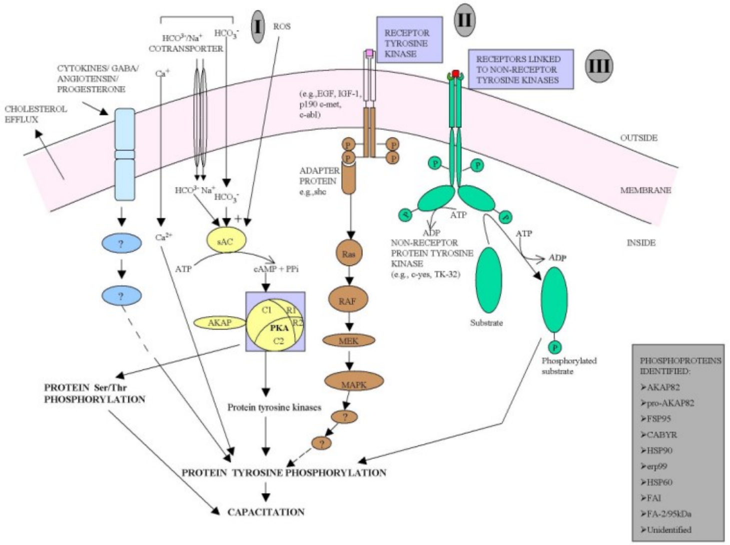
I
ROS
HCO3-/Na+ COTRANSPORTER
HCO3-
CYTOKINES/ GABA/ ANGIOTENSIN/ PROGESTERONE
CHOLESTEROL EFFLUX
Ca+
Ca2+
sAC
ATP
cAMP + PPi
AKAP
PKA
C1
C2
R1
R2
PROTEIN Ser/Thr PHOSPHORYLATION
Protein tyrosine kinases
PROTEIN TYROSINE PHOSPHORYLATION
CAPACITATION
II
RECEPTOR TYROSINE KINASE
(e.g.,EGF, IGF-1, p190 c-met, c-abl)
ADAPTER PROTEIN e.g.,shc
Ras
RAF
MEK
MAPK
III
RECEPTORS LINKED TO NON-RECEPTOR TYROSINE KINASES
ADP
NON-RECEPTOR PROTEIN TYROSINE KINASE (e.g., c-yes, TK-32)
Substrate
Phosphorylated substrate
OUTSIDE
MEMBRANE
INSIDE
PHOSPHOPROTEINS IDENTIFIED:
AKAP82
pro-AKAP82
FSP95
CABYR
HSP90
erp99
HSP60
FAI
FA-2/95kDa
Unidentified

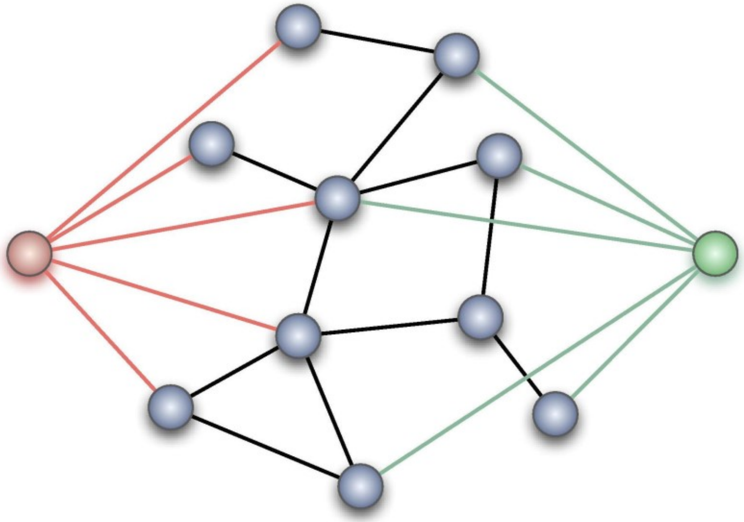

The link

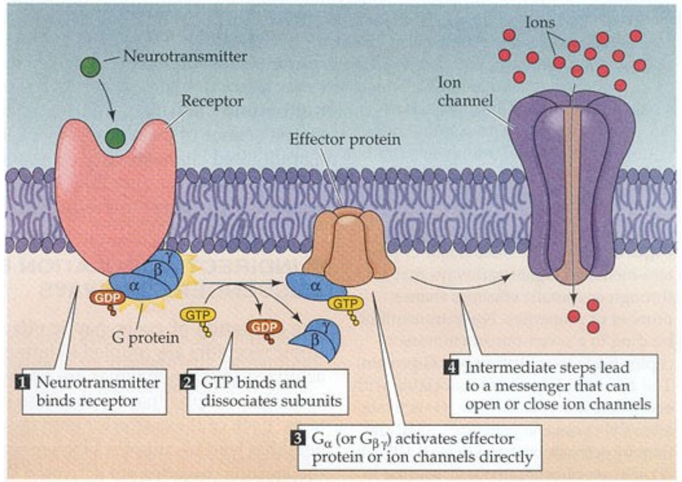
Ions
Neurotransmitter
Receptor
Ion channel
Effector protein
G protein
GDP
GTP
1 Neurotransmitter binds receptor
2 GTP binds and dissociates subunits
3 G_α (or $G_{\beta\gamma}$) activates effector protein or ion channels directly
4 Intermediate steps lead to a messenger that can open or close ion channels

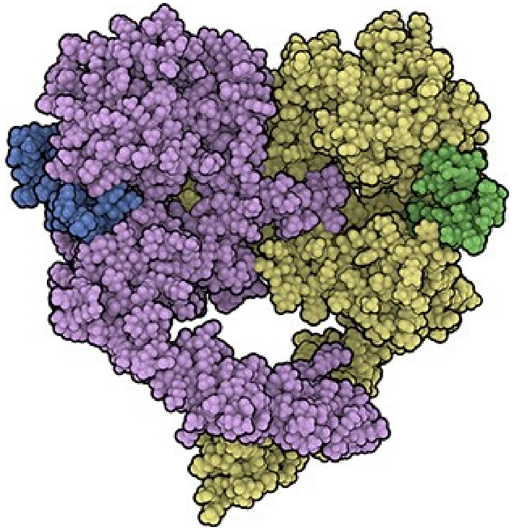

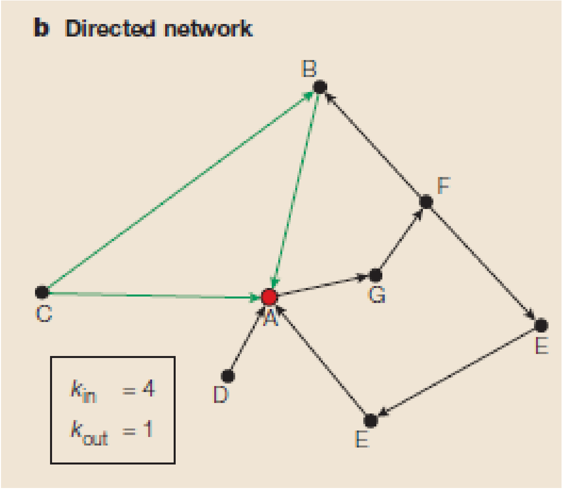
b Directed network
B
F
C
A
G
D
E
E
k_{in} = 4
k_{out} = 1

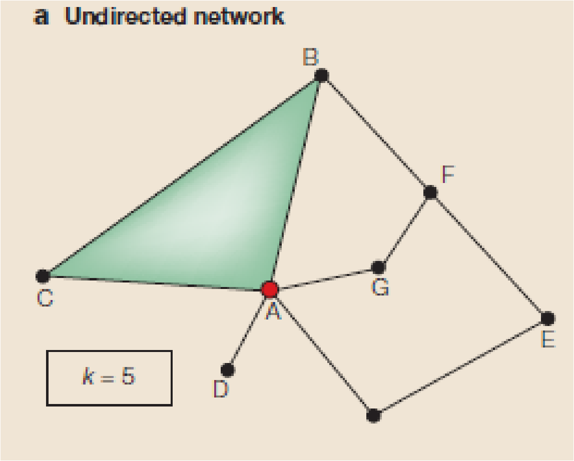
a Undirected network
B
F
C
A
G
D
E
k = 5

NETWORK NAME	NODES	LINKS	DIRECTED/ UNDIRECTED	N	L	‹K›
Internet	routers	Internet Connections	Undirected	192,244	609,066	2.67
WWW	webpages	links	Directed	325,729	1,497,134	4.60
Power Grid	power plants, transformers	cables	Undirected	4,941	6,594	2.67
Mobile-Phone Calls	subscribers	calls	Directed	36,595	91,826	2.51
Email	email addresses	emails	Directed	57,194	103,731	1.81
Science Collaboration	scientists	co-authorships	Undirected	23,133	186,936	16.16
Actor Network	actors	co-acting	Undirected	212,250	3,054,278	28.78
Citation Network	papers	citations	Directed	449,673	4,707,958	10.47
E. coli Metabolism	metabolites	chemical reactions	Directed	1,039	5,802	5.84
Yeast Protein Interactions	proteins	binding interactions	Undirected	2,018	2,930	2.90

Table 2.1

Network maps and their basic properties.

Network topology

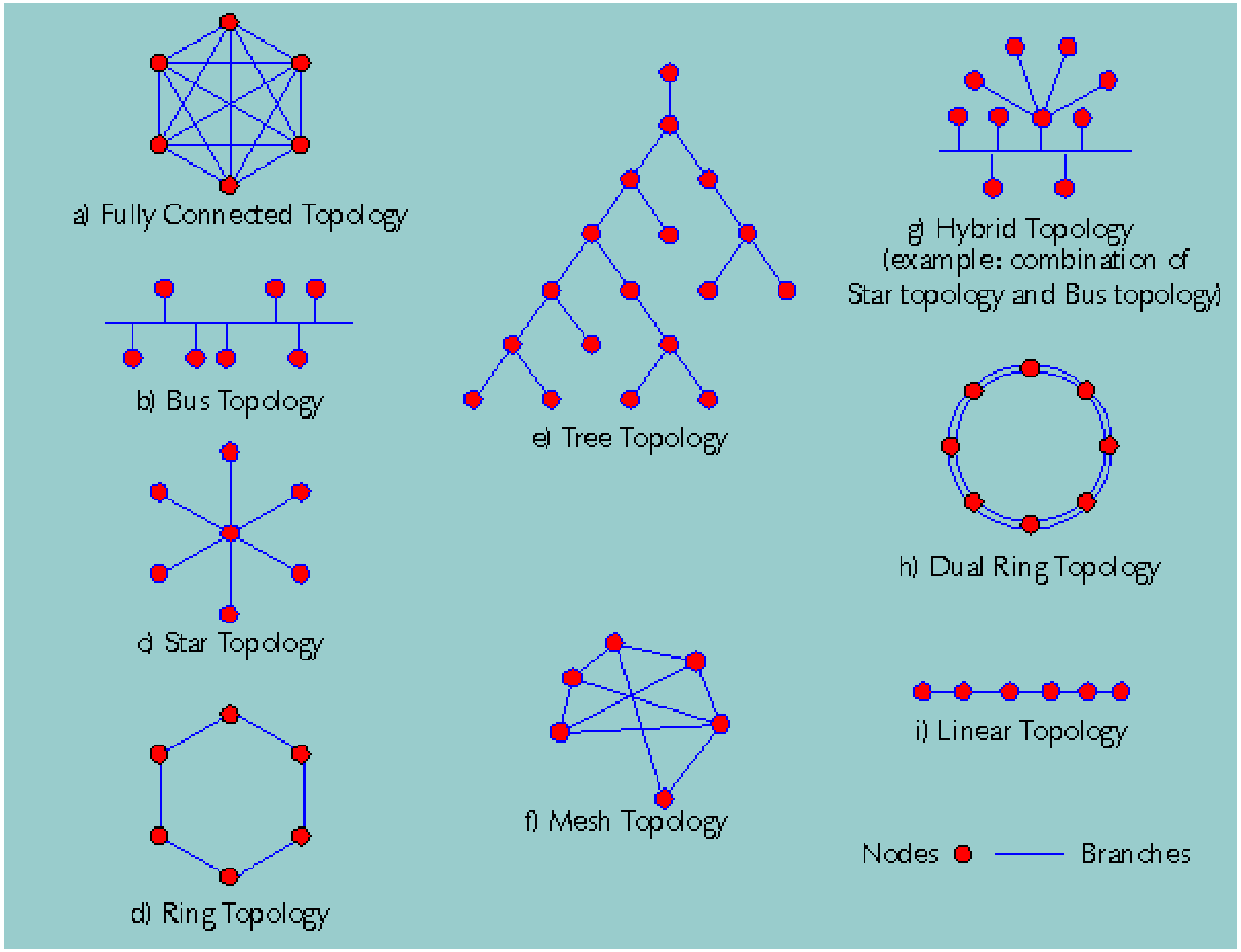

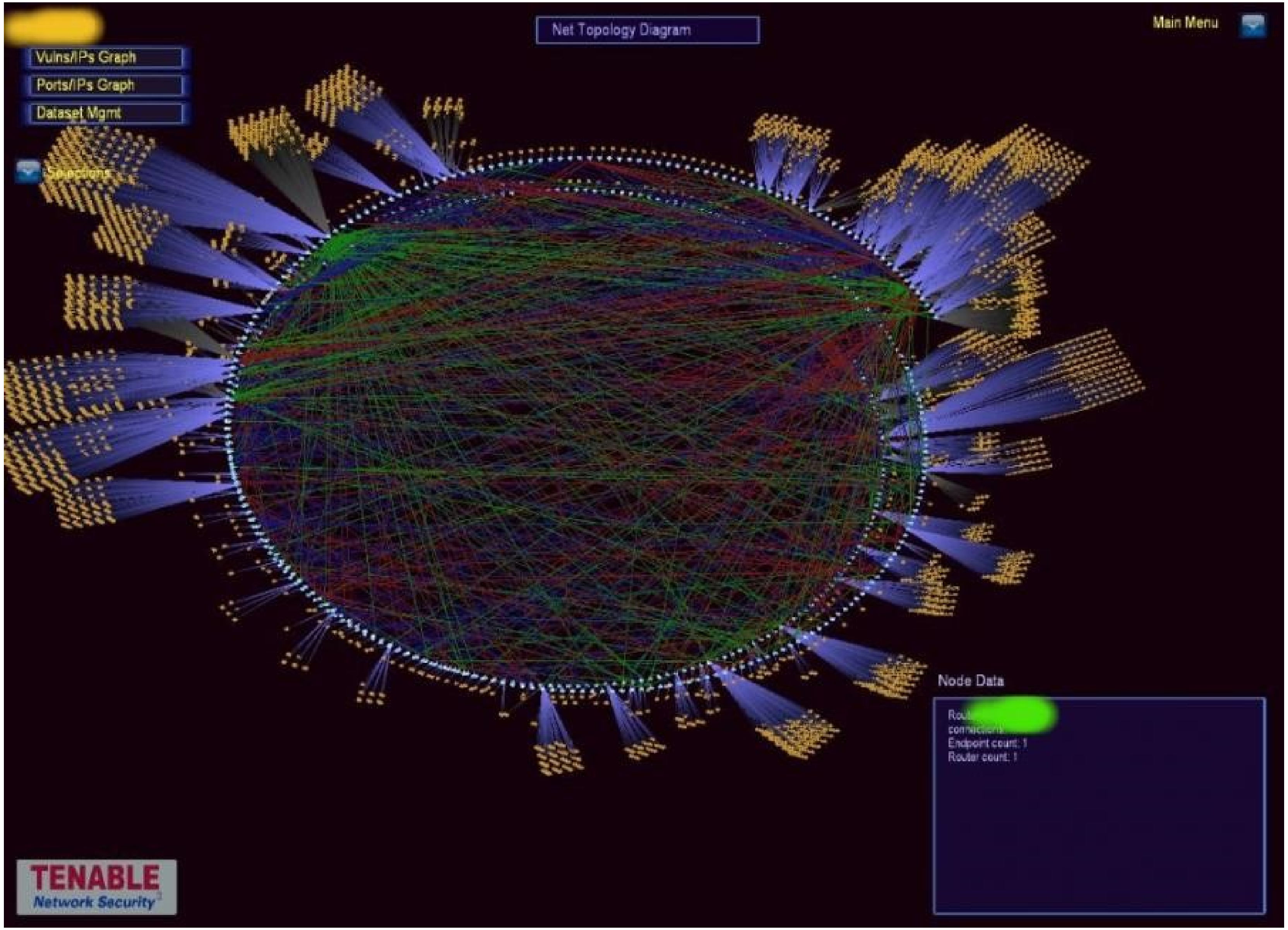
Net Topology Diagram
Main Menu
Vulns/IPs Graph
Ports/IPs Graph
Dataset Mgmt
Node Data
Endpoint count: 1
Router count: 1
TENABLE
Network Security

Network Topology

the number of nodes: which represents the total number of molecules involved;

In an undirected network total number of links, L, can be expressed as the sum of the node degrees:

$$L = \frac{1}{2}\sum_{i=1}^{N} k_i \qquad (1)$$

Here the 1/2 factor corrects for the fact that in the sum (1) each link is counted twice.

the number of edges: which represents the total number of interaction among nods within the network;

the node degree (or connectivity): which indicates how many links each node has to other nodes;

$$\langle k \rangle \equiv \frac{1}{N}\sum_{i=1}^{N} k_i = \frac{2L}{N} \qquad (7)$$

In directed networks we distinguish between *incoming degree*, k_i^{in}, representing the number of links that point node i, and *outgoing degree*, k_i^{out}, representing the number of links that point from the node i to other nodes and the *total degree*, k_i, given by

$$k_i = k_i^{in} + k_i^{out} \qquad (8)$$

the node degree distribution P(k): which represents the probability that a selected node has exactly *k* links;

$$p_k = \frac{N_k}{N}$$

the clustering coefficient: it is a measure of how the nodes tend to form clusters: the more the clustering coefficient is higher, the more the presence of clusters will increase;

$$C_I = 2n_I/k(k-1),$$

where n_I is the number of links connecting the k_I neighbours of node I to each other

clustering coefficient

$$C = \frac{3 \times \text{number of triangles}}{\text{number of connected triples of vertices}} =$$

$$= \frac{\text{number of closed triplets}}{\text{number of connected triples of vertices}}.$$

$$\bar{C} = \frac{1}{n} \sum_{i=1}^{n} C_i .$$

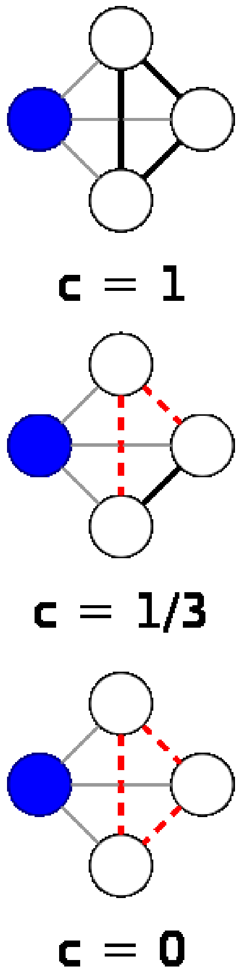

the network diameter: which is the largest distance between two nodes;

the averaged number of neighbours: which is the mean number of connection of nodes;

the characteristic path length: which is the expected distance between two random individuated connected nodes.

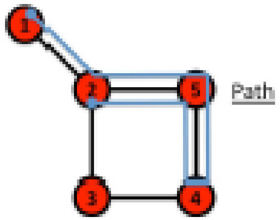

PATH: A sequence of nodes such that each node is connected to the next node along the path by a link. A path always consists of n nodes and $n - 1$ links. The length of a path is defined as the number of its links, counting multiple edges multiple times.

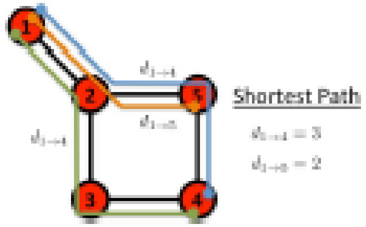

SHORTEST PATH (geodesic path, d): the path with the shortest distance d between two nodes. We will call it the distance between two nodes.

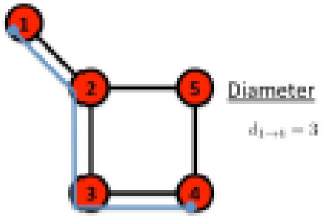

DIAMETER (d_{max}): the longest shortest path in a graph, or the distance between the two furthest away nodes.

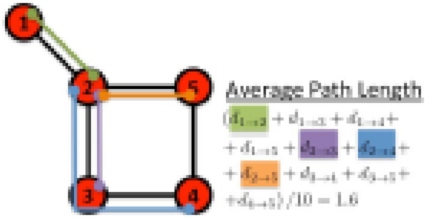

AVERAGE PATH LENGTH ($\langle d \rangle$): the average of the shortest paths between all pairs of nodes.

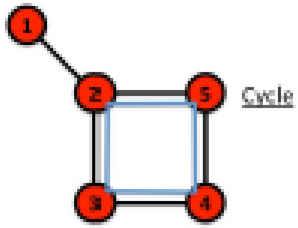

CYCLE: a path with the same start and end node.

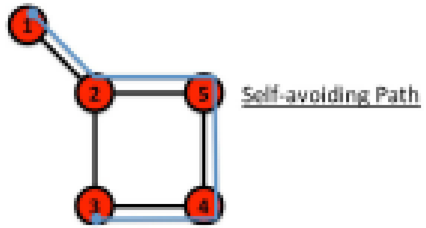

SELF-AVOIDING PATH: a path that does not intersect itself, i.e. the same node or link does not occur twice along the path.

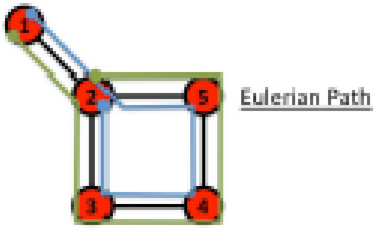

EULERIAN PATH: a path that traverses each link exactly once.

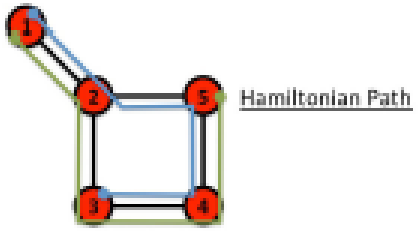

HAMILTONIAN PATH: a path that visits each node exactly once.

The tripartite recipe–ingredient–compound network, in which one set of nodes are recipes, like Chicken Marsala, the second set corresponds to the ingredients each recipe has (like flour, sage, chicken, wine, and butter for Chicken Marsala), and the third set captures the flavor compounds, or chemicals that contribute to the taste of a particular ingredient.

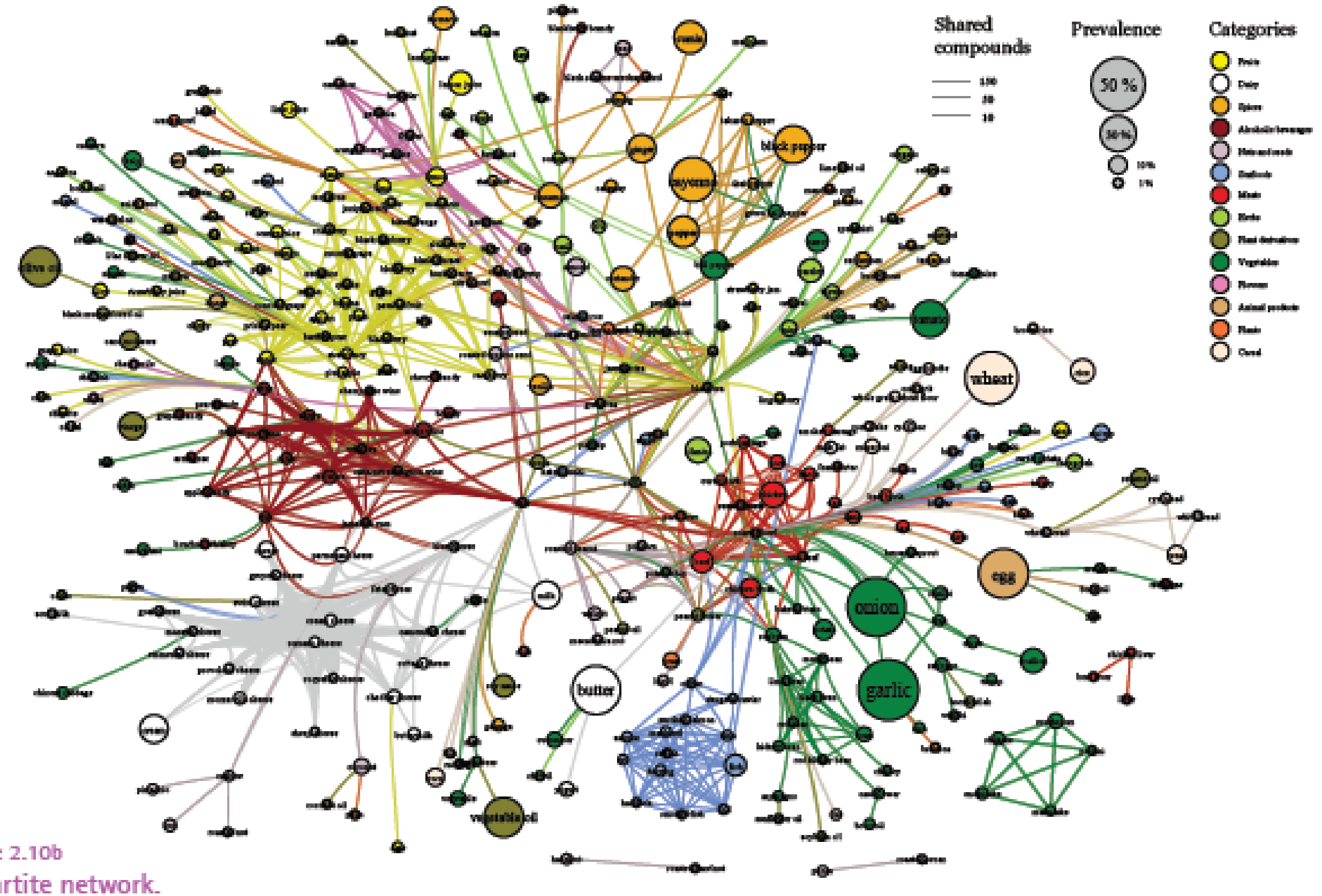

Image 2.10b
Tripartite network.

A projection of the tripartite network, resulting in the ingredient network, often called the flavor network. Each node denotes an ingredient; the node color indicating the food category and node size reflects the ingredient prevalence in recipes. Two ingredients are connected if they share a significant number of flavor compounds, link thickness representing the number of shared compounds between the two ingredients (After [12]).

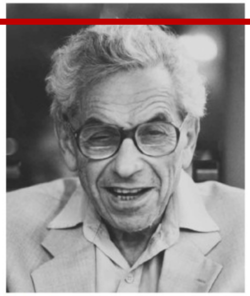

Image 3.2a
Pál Erdős (1913–1996)

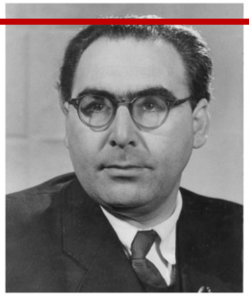

Image 3.2b
Alfréd Rényi (1921–1970)

Erdős–Rényi model

sets an edge between each pair of nodes with equal probability, independently of the other edges

G(*n*,*p*)

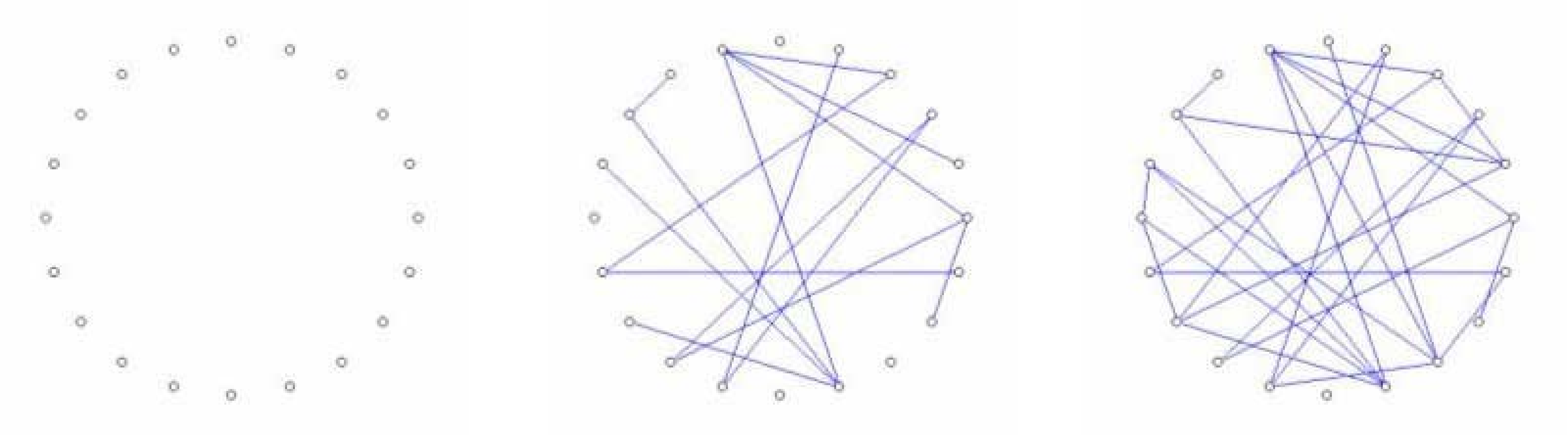

$p = 0$ (a) $p = 0.1$ (b) $p = 0.2$ (c)

Random networks

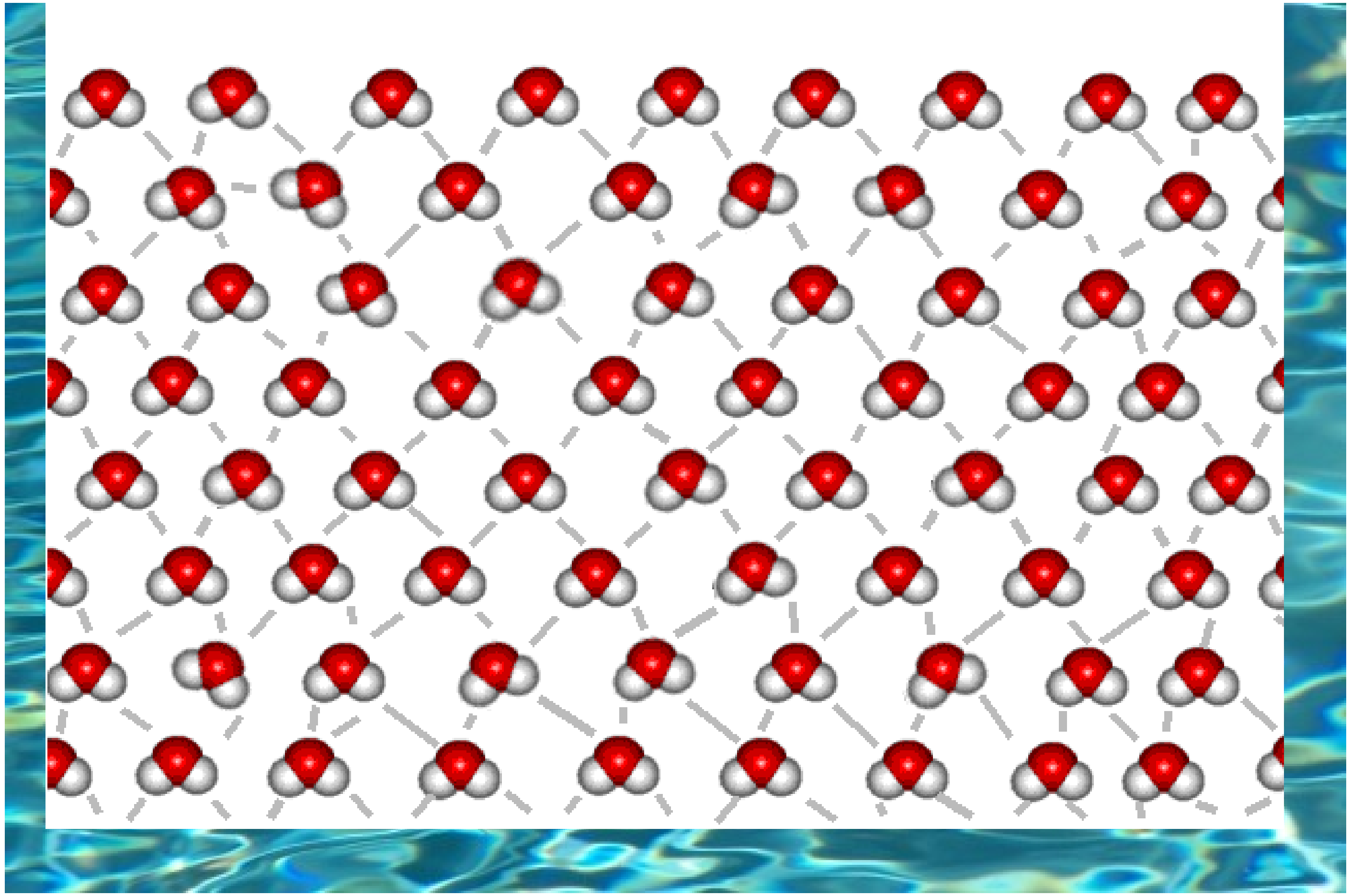

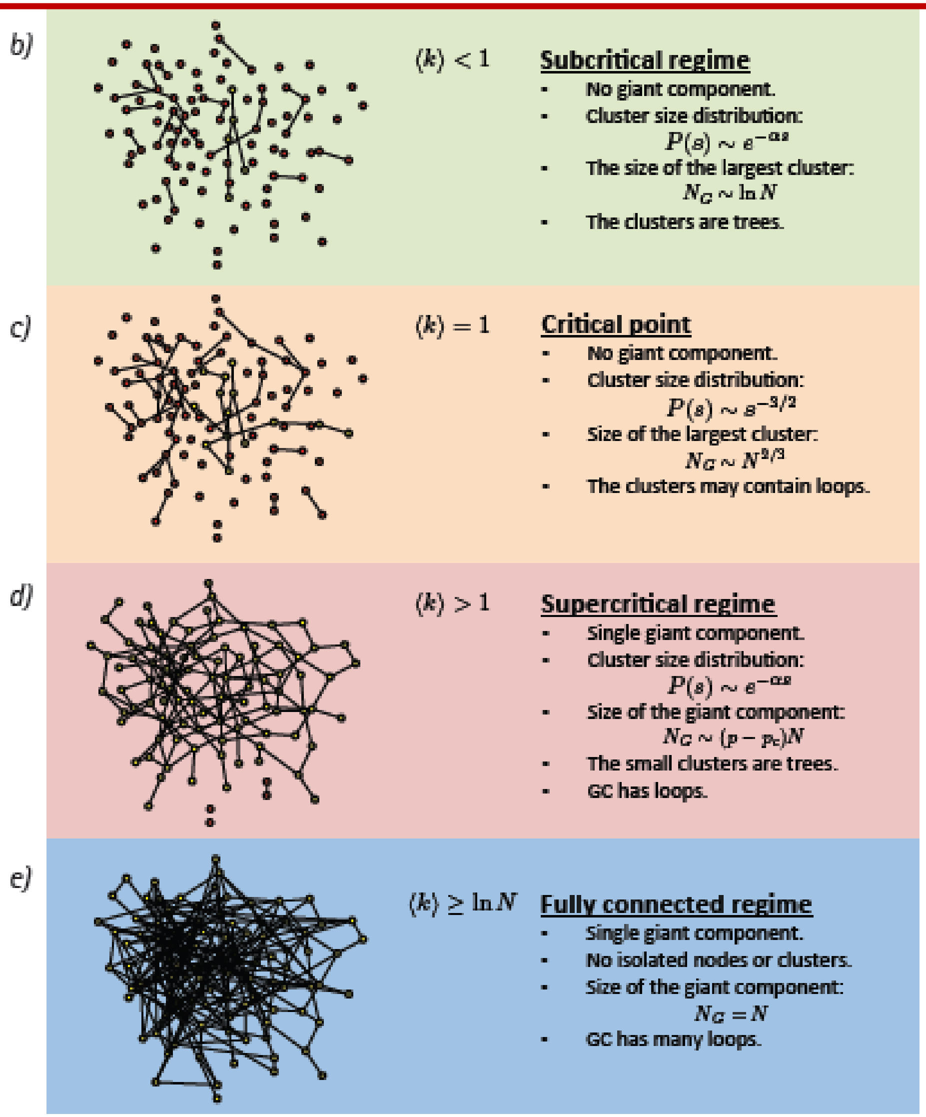

Image 3.6

Evolution of a random network.

(a) The relative size of the giant component in function of the average degree $\langle k \rangle$ in the Erdős-Rényi model.
(b)-(e) The main network characteristics in the four regimes that characterize a random network.

Watts and Strogatz model

- However the ER graphs do not have two important properties observed in many real-world networks:
- They do not generate local clustering and triadic closures. Instead because they have a constant, random, and independent probability of two nodes being connected, ER graphs have a low clustering coefficient.

Small wolrd

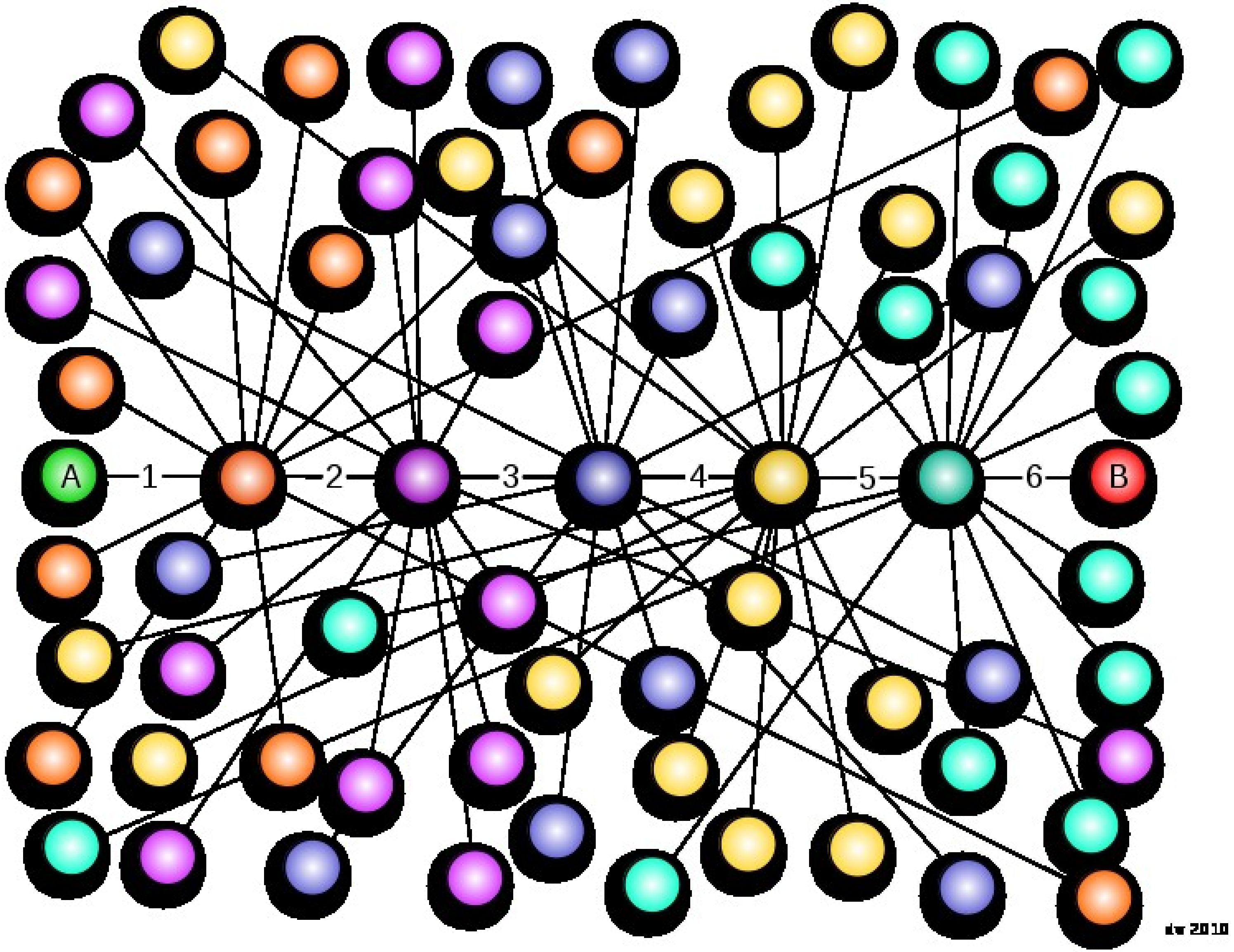

Six degree of separation

Milgram experiment

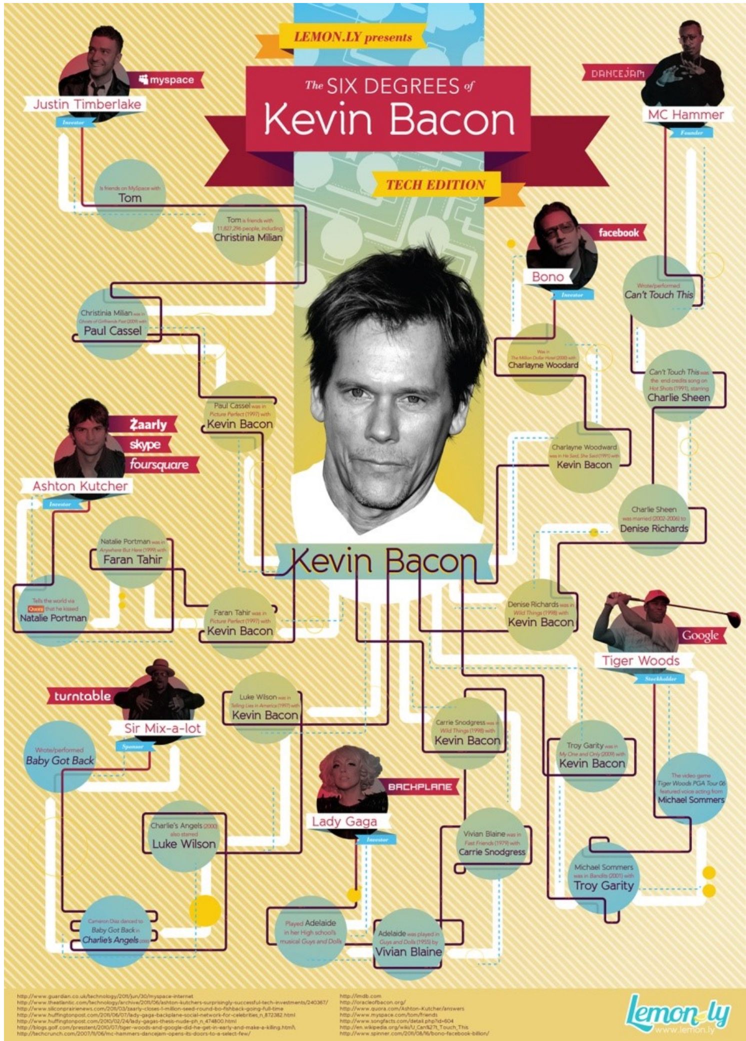

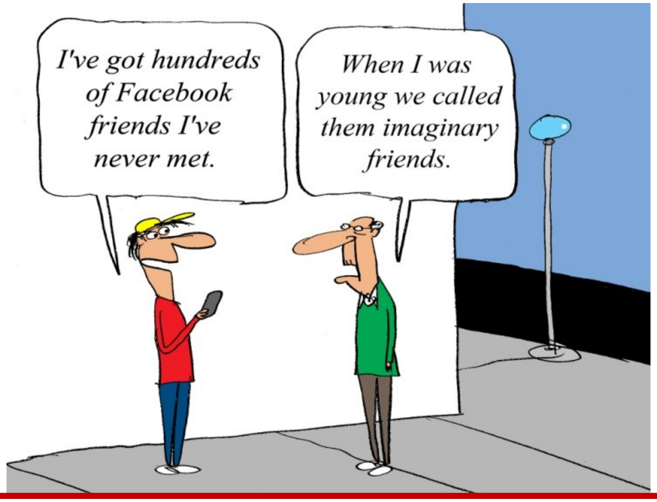

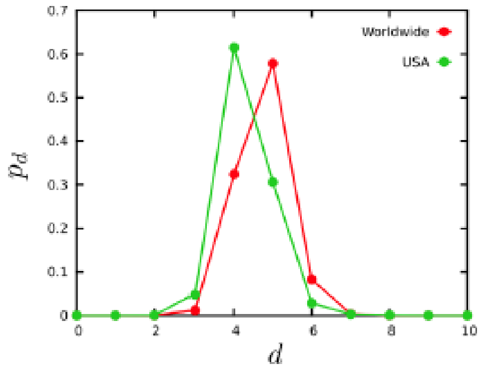

Image 3.11

Six degrees? Facebook finds only four.

Milgram's experiment could not detect the true distance between his study's participants, as he lacked an accurate map of the full social network. Today Facebook has the most extensive social network map ever assembled. Using Facebook's social graph of May 2011, consisting of 721 million active users and 68 billion symmetric friendship links, the average distance between the users was 4.74. The figure shows the distance distribution, p_d, for all pairs of Facebook users worldwide (full dataset) and within the US only. Therefore, instead of 'six degrees' researchers detected only 'four degrees of separation' [4], closer to the prediction of Eq. (20) than to Milgram's six degrees [23]. Using Facebook's N and L Eq. (19) predicts the average degree to be approximately 3.90, not far from the reported four degrees.

The hubs

Barabasi-Albert model

- Node degree: $\mathbf{y} = a\,\mathbf{x}^{-b}$

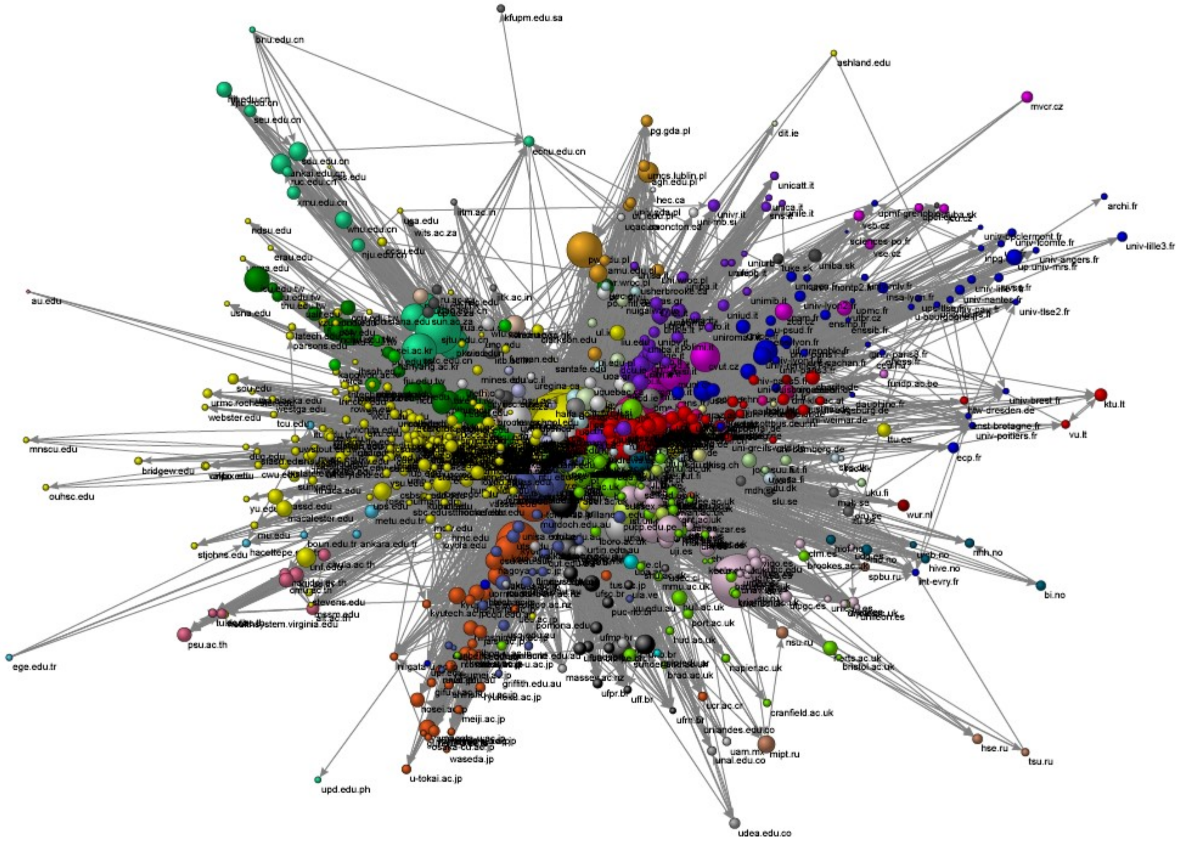

transportation

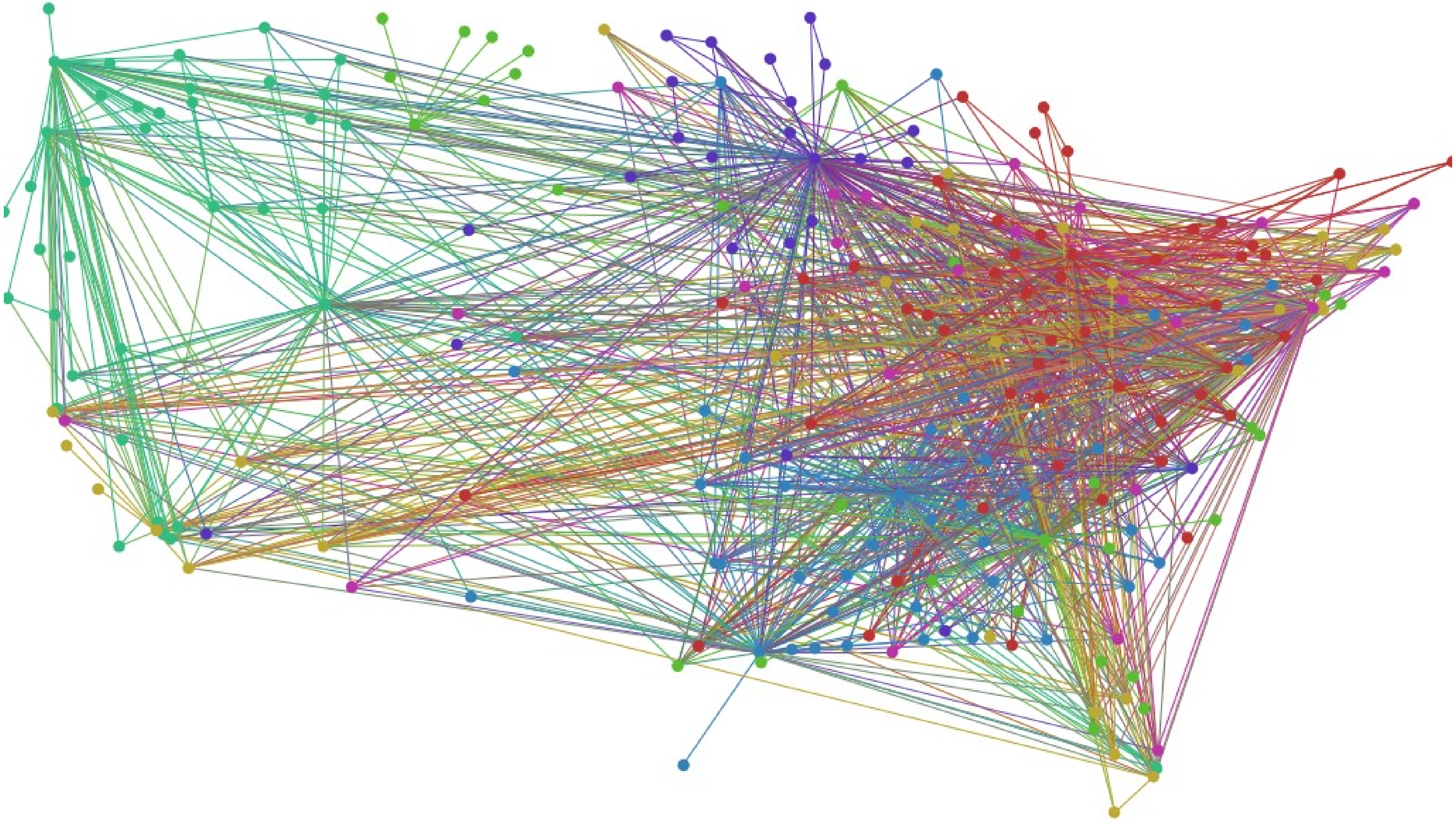

A biological example…

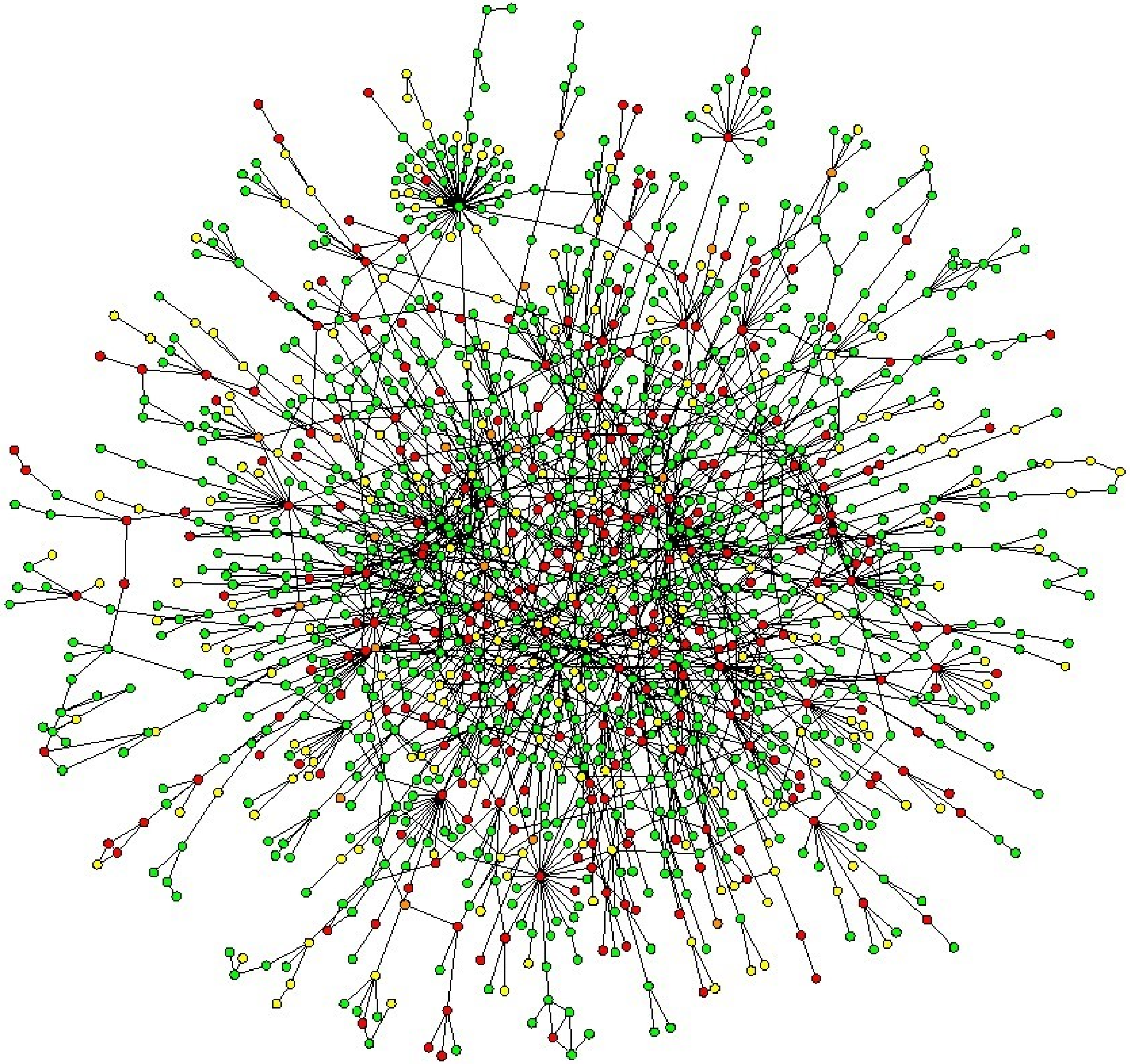

Robustness against random attacks

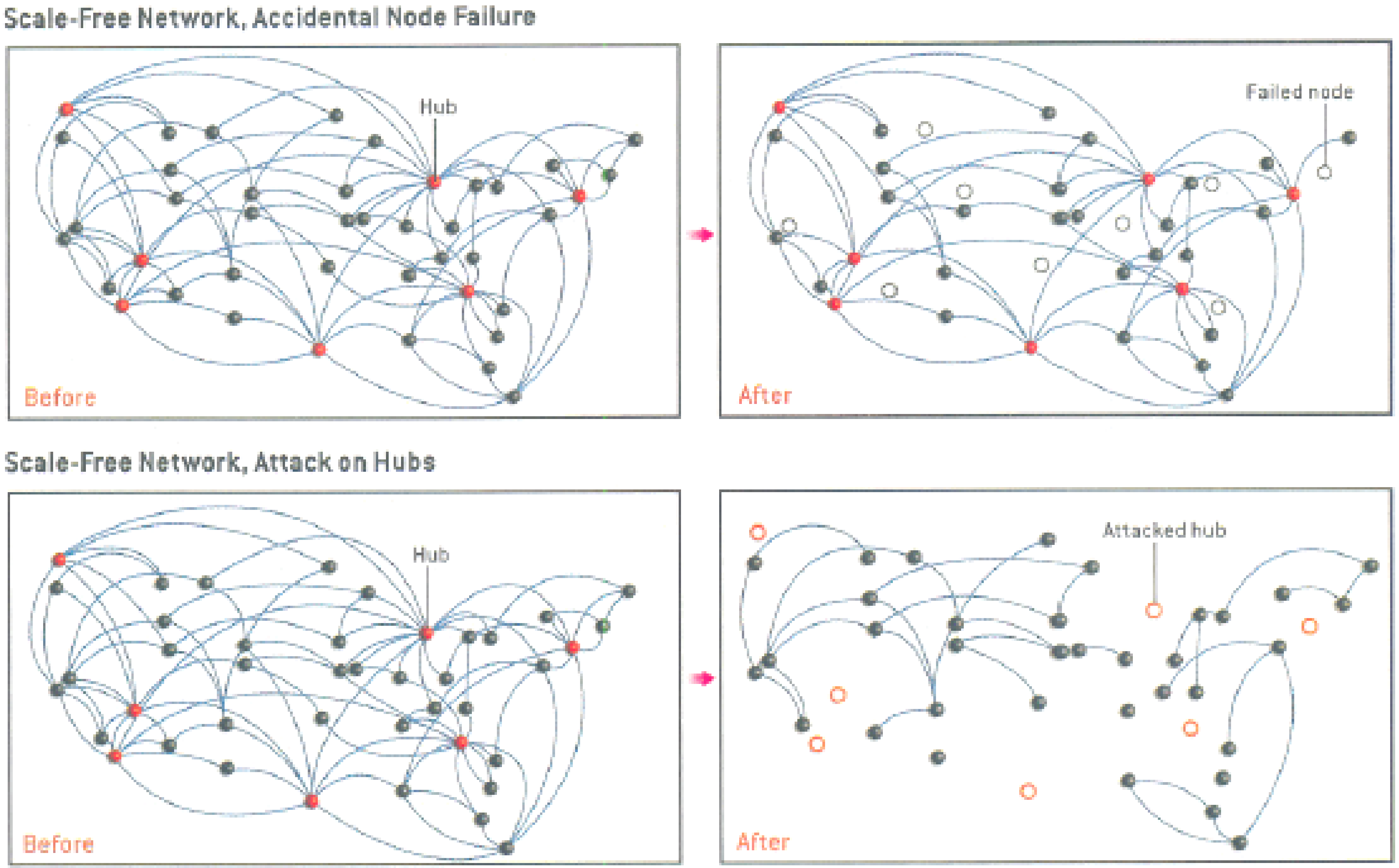

… in conclusion

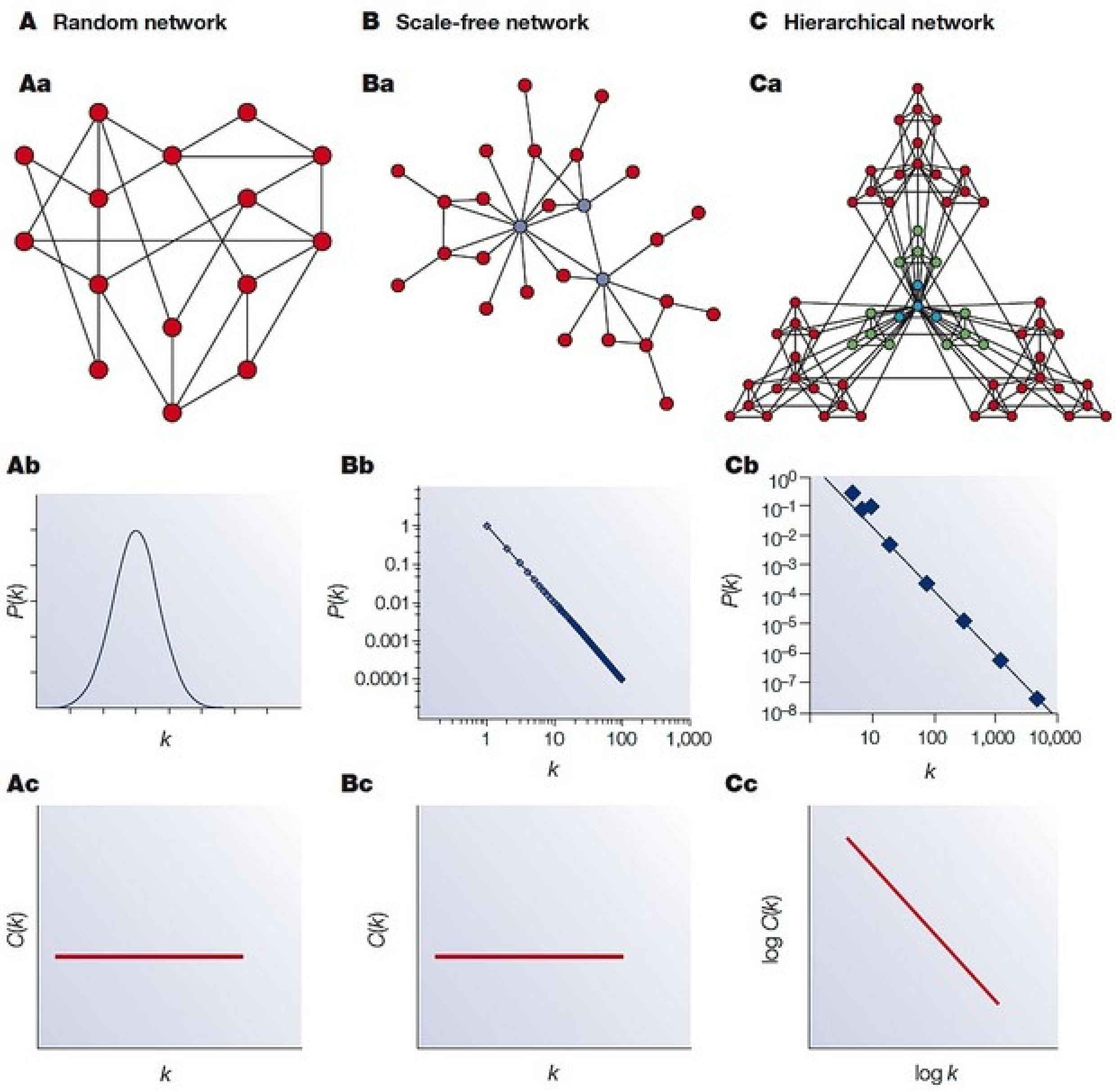

Going back to fertilization

Biological Networks biology and reproduction

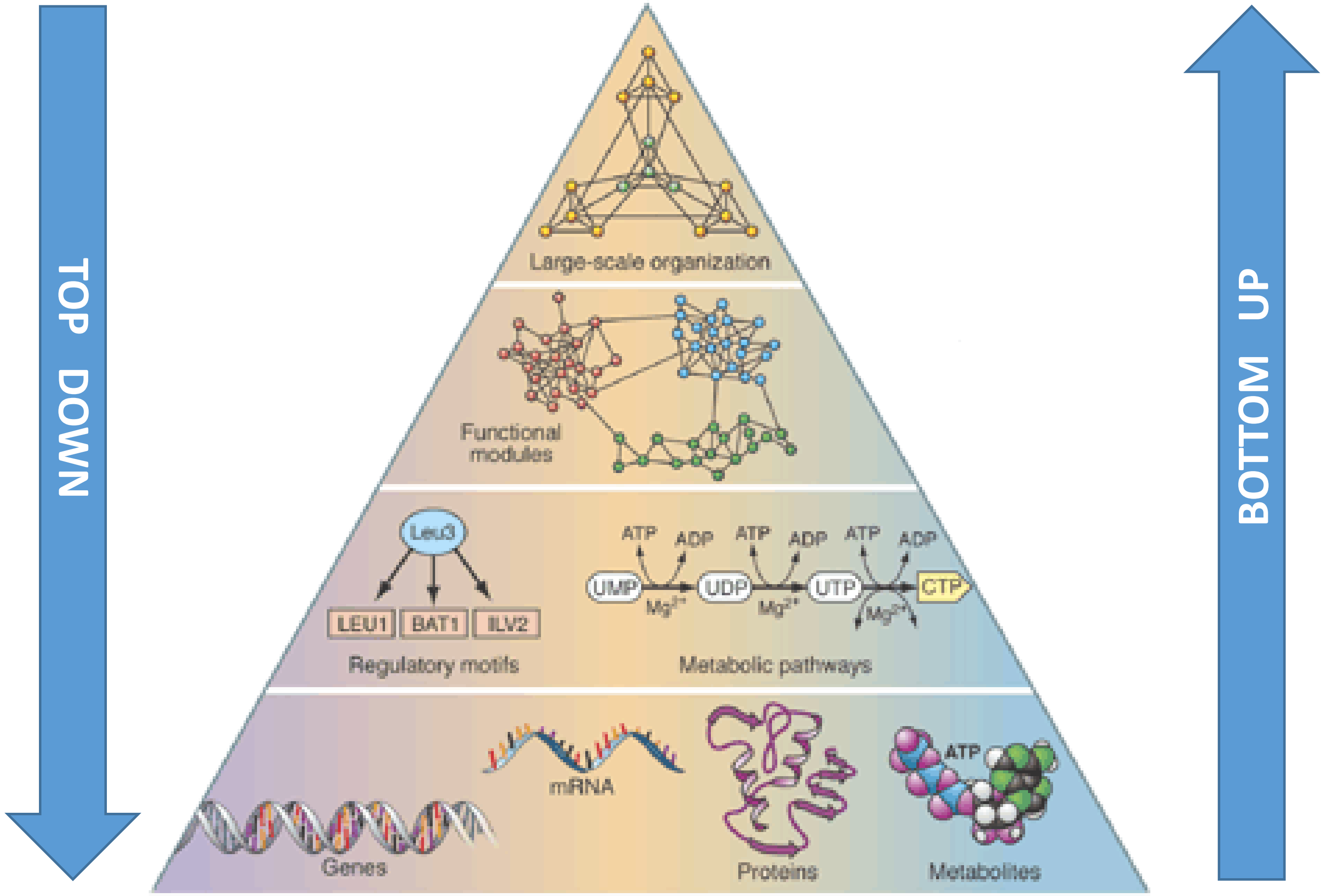

The model


Bernabò et al. BMC Systems Biology 2010, 4:87
http://www.biomedcentral.com/1752-0509/4/87

BMC Systems Biology

RESEARCH ARTICLE Open Access

The spermatozoa caught in the net: the biological networks to study the male gametes post-ejaculatory life

Nicola Bernabò*, Mauro Mattioli and Barbara Barboni

Highly accessed

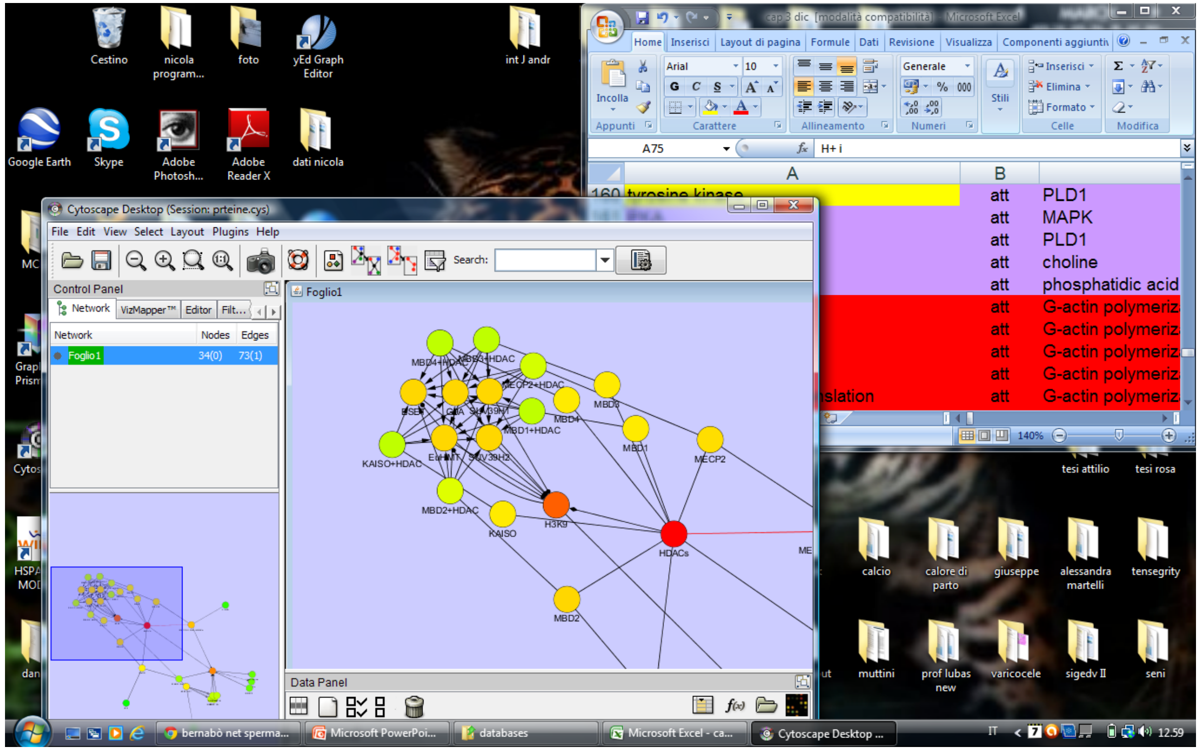

The networks

Capacitaton

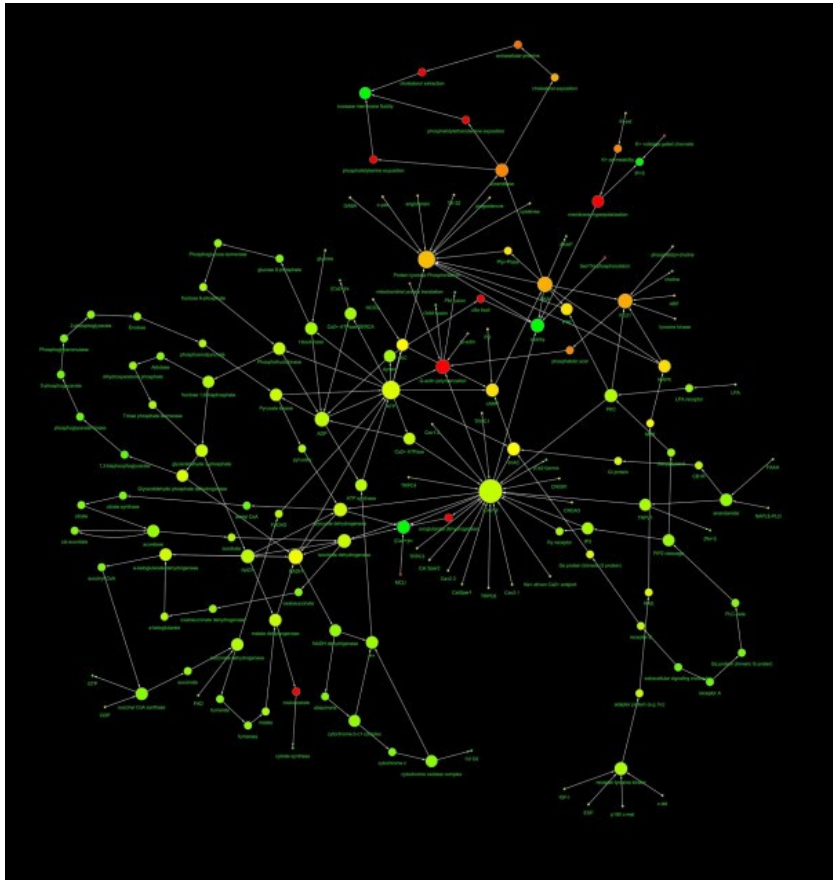

Acrosome reaction

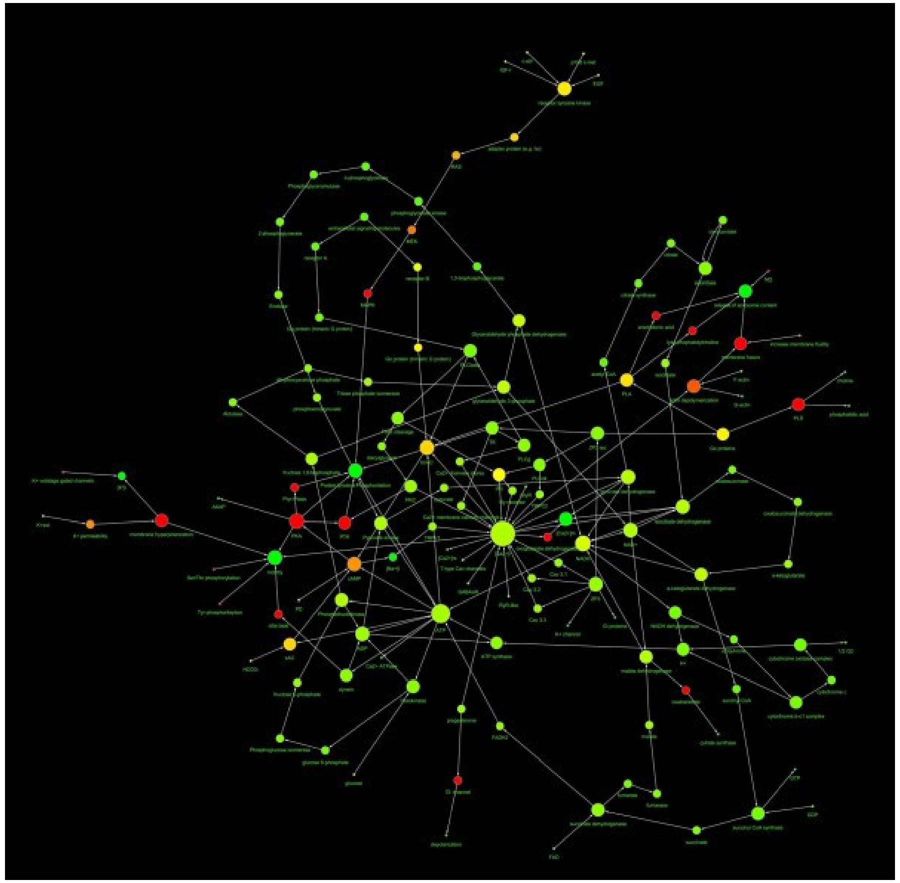

Networks topology

Table 1: Main topological parameters of capacitation and AR networks

	capacitation	AR
N°nodes	146	141
N°edges	197	191
Clustering coefficient	0.029	0.026
Diameter	20	20
Averaged n°neighbours	2.667	2.695
Char. path length	6.606	6.736

The number of nodes represent the total number of molecules involved, the number of edges represents the total number of interaction found, the clustering coefficient is calculated as $CI = 2nI/k(k-1)$, where nI is the number of links connecting the kI neighbours of node I to each other, the network diameter is the largest distance between two nodes, the Averaged n°neighbours represent the mean number of connection of each node, the Char. path length gives the expected distance between two connected nodes.

Table 2: Result of power law fitting of IN and OUT capacitation and AR networks

	capacitation		AR	
	in	out	in	out
r	0.992	0.997	0.992	0.989
R^2	0.897	0.837	0.906	0.823
b	-1.547	-2.046	-1.657	-2.303

Table 3: Most connected nodes (the hubs) of capacitation and AR networks

Network	Node	Number of links
capacitation	$[Ca^{2+}]_i$	25
capacitation	ATP	14
capacitation	Tyr phosphorylation	13
capacitation	PKA	9
capacitation	ADP	8
capacitation	PLD1	8
AR	$[Ca^{2+}]_i$	23
AR	ATP	13

Hubs removal

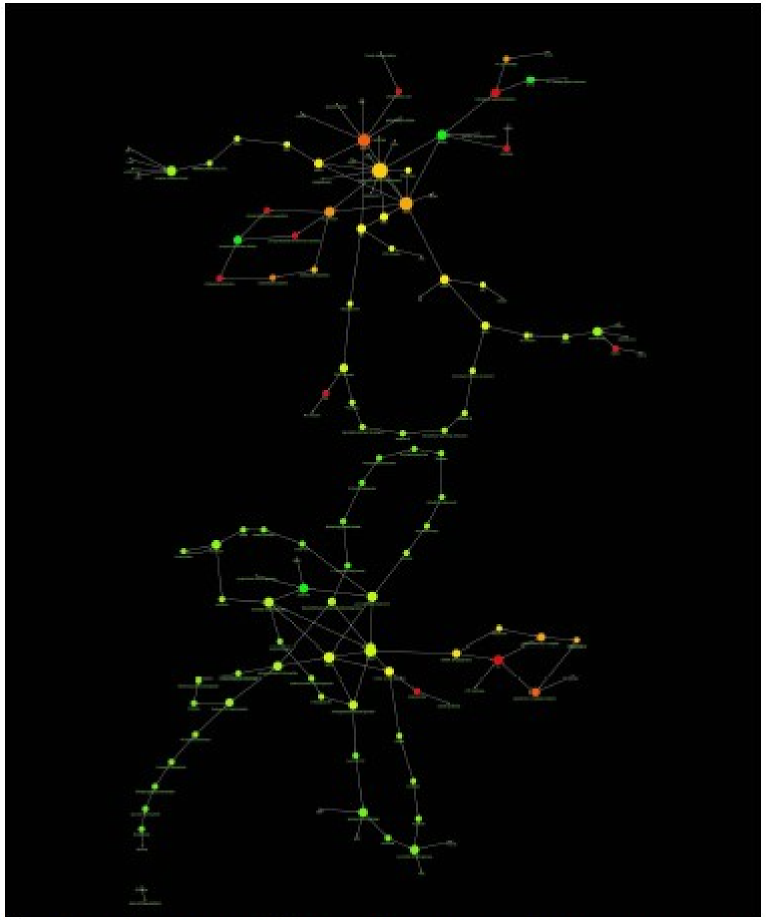

Figure 4 Diagram showing the effect of the elimination from capacitation network of the most linked nodes. The elimination from capacitation network of the most linked nodes ($[Ca^{2+}]_i$ and ATP-ADP) caused the collapse of network structure.

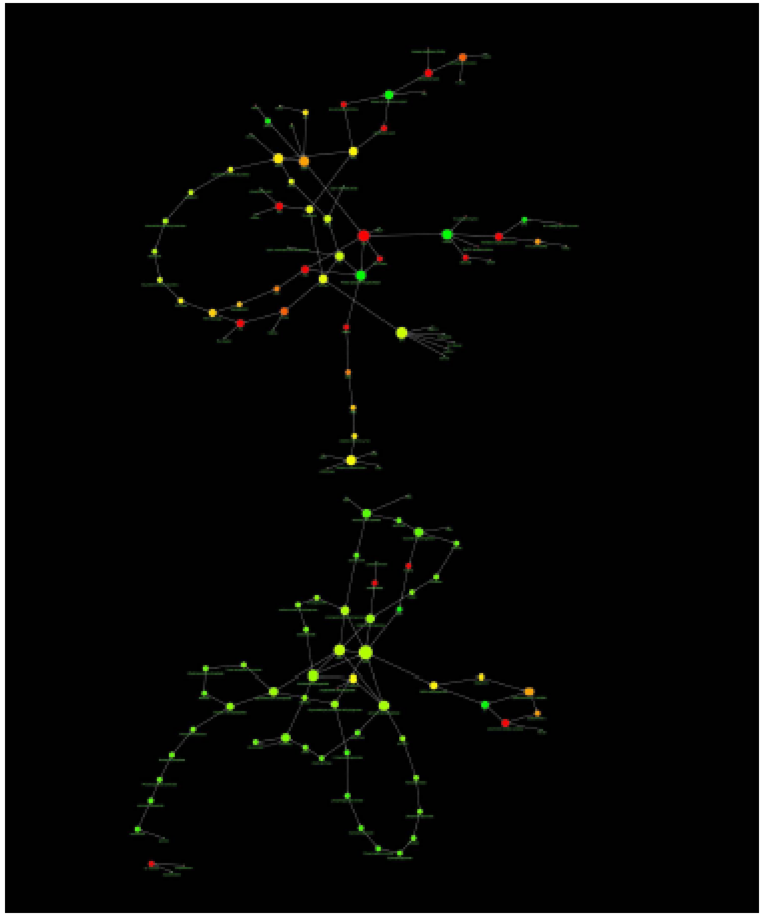

Figure 5 Diagram showing the effect of the elimination from AR network of the most linked nodes. The elimination from AR network of the most linked nodes ($[Ca^{2+}]_i$ and ATP-ADP) caused the collapse of network structure.

Common elements

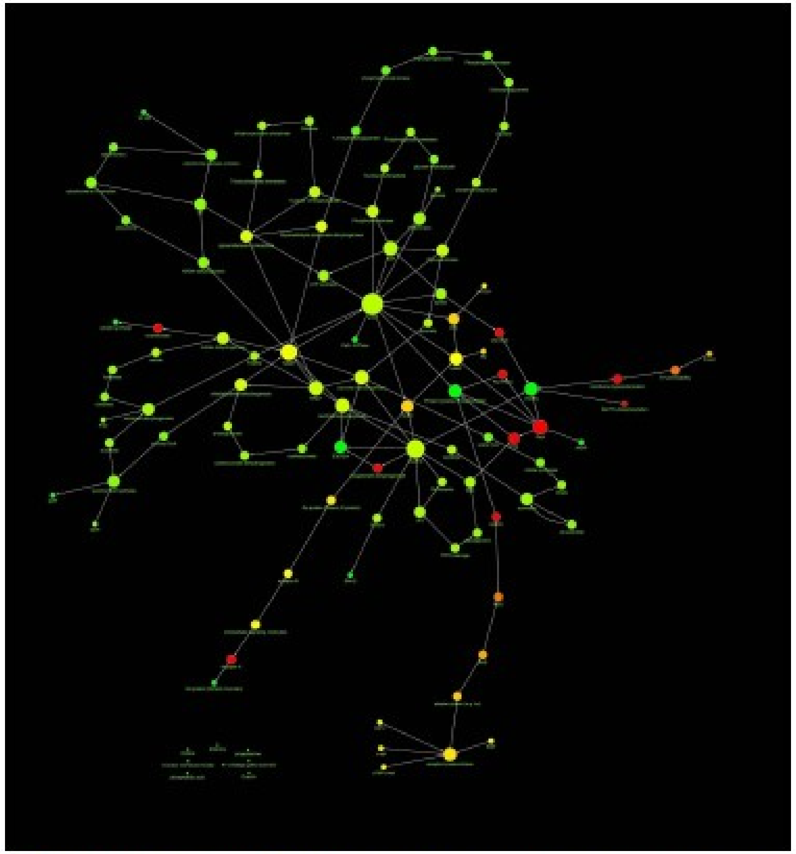

Figure 3 Diagram showing the structure of the C A network. The nodes diameter is proportional to the number of links, the color varies depending on the network centrality. The direction of arrows represents the direction of the interaction (from the source to the target). The spatial network arrangement was obtained by using the Cytoscape Spring-embedded Layout (see the text for explanation).

Table 4: Main topological parameters and the most connected nodes of C A network

	C A
N°nodes	109
N°edges	143
Clustering coefficient	0.036
Diameter	20
Averaged n°neighbours	2.606
Char. path length	6.957
IN degree distribution	b = -1.829 r = 0.997 $R^2 = 0.948$
OUT degree distribution	b = -2.240 r = 0.992 $R^2 = 0.894$
Hub (n°edges)	ATP (13); Ca^{2+} (12)

The number of nodes represent the total number of molecules involved, the number of edges represents the total number of interaction found, the clustering coefficient is calculated as $CI = 2nI/k(k-1)$, where nI is the number of links connecting the kI neighbours of node I to each other, the network diameter is the largest distance between two nodes, the Averaged n°neighbours represent the mean number of connection of each node, the Char. path length gives the expected distance between two connected nodes.

Consequently …

- It is possible to represent the biological events involved in reproduction as networks models;
- They are scale free networks;
- The have a ultra small-world topology;
- It is possible to take important inerences.

Experimental validation of the model

Bernabò *et al. BMC Systems Biology* 2011, 5:47
http://www.biomedcentral.com/1752-0509/5/47

BMC Systems Biology

RESEARCH ARTICLE Open Access

The role of actin in capacitation-related signaling: an in silico and in vitro study

Nicola Bernabò*, Paolo Berardinelli, Annunziata Mauro, Valentina Russo, Pia Lucidi, Mauro Mattioli and Barbara Barboni

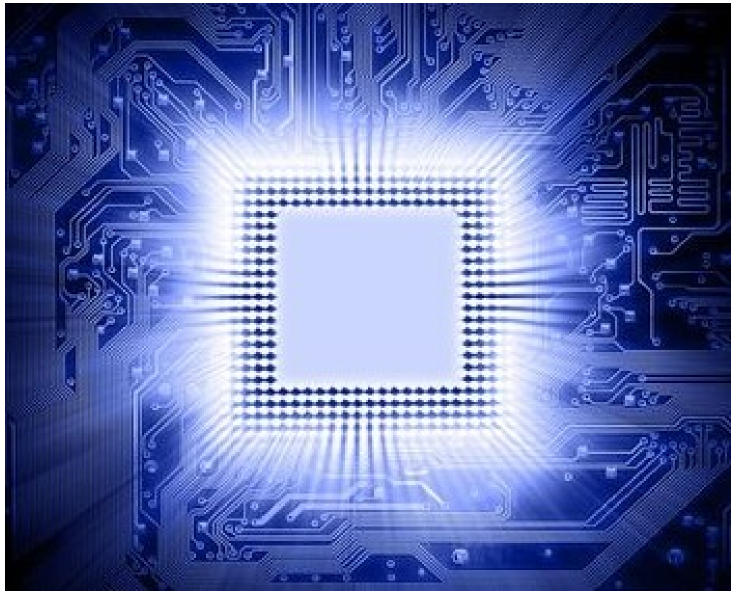

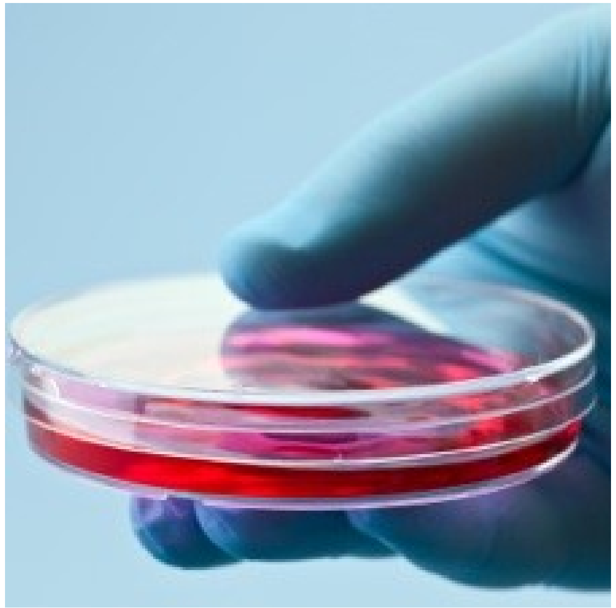

Organization of signalig systems

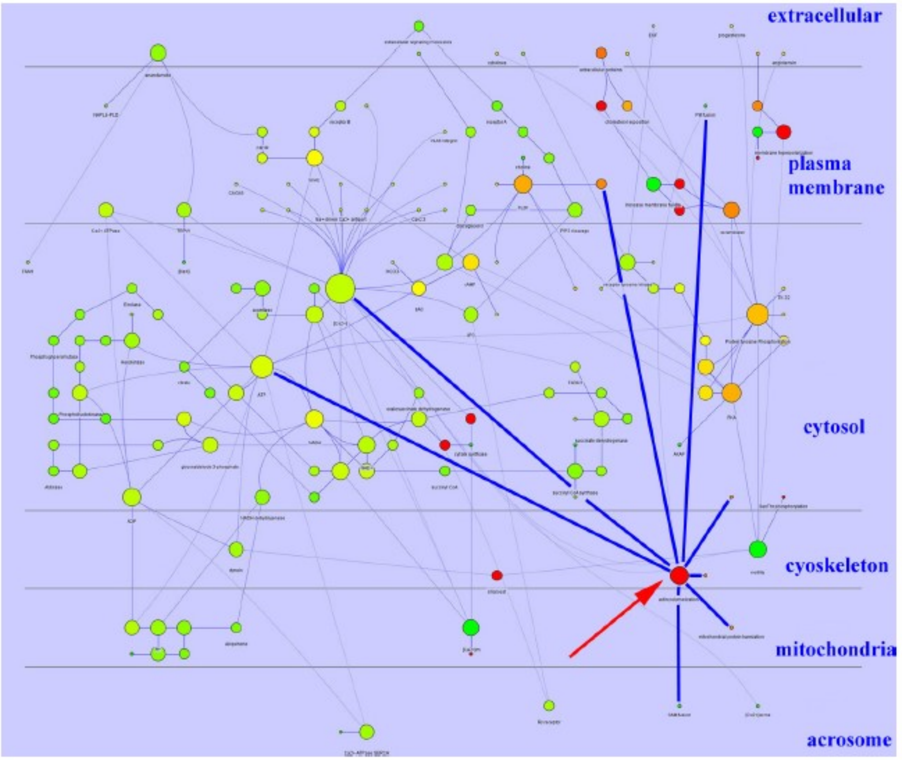

Figure 1 Diagram showing the structure of the boar spermatozoa capacitation network and the subcellular localization of nodes. The node size was proportional to the connection number and the node color gradient was dependent from the closeness centrality. This parameter is computed as: $C_c(n) = 1/avg(L(n,m))$, were L (n,m) is the length of the shortest path between two nodes *n* and *m*. The closeness centrality of each node ranges from 0 (red) to 1 (green) and it is a measure of how fast the information spreads from a given node to the other nodes. The actn polymerization node is indicated by the red arrow, its links by blue line. All the nodes were localized in their specific subcellular domain (Cerebral V.2).

Table 2 Most connected nodes (the hubs) of capacitation network

Node	Number of links
$[Ca^{2+}]_i$	28
ATP	15
Tyr phosphorylation	13
PKA	9
ADP	8
PLD1	8
NADH	8
Actin polymerization	8

Membrane fusion is impossible

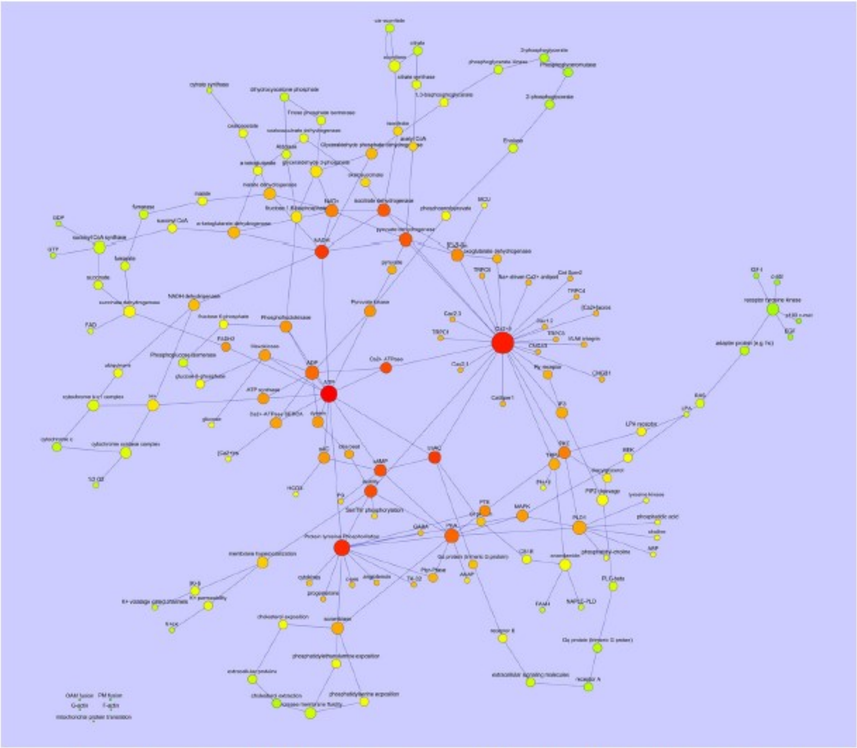

Figure 2 Diagram showing the structure of the boar spermatozoa capacitation network after "actin polymerization" node removal. The node size was proportional to the connection number and the node color gradient was dependent from the closeness centrality. This parameter is computed as: $C_c(n) = 1/avg(L(n,m))$, were L (n,m) is the length of the shortest path between two nodes *n* and *m*. The closeness centrality of each node ranges from 0 (red) to 1 (green) and it is a measure of how fast the information spreads from a given node to the other nodes. The spatial network arrangement was obtained by using the Cytoscape Spring-embedded Layout (see the text for explanation).

F-actin

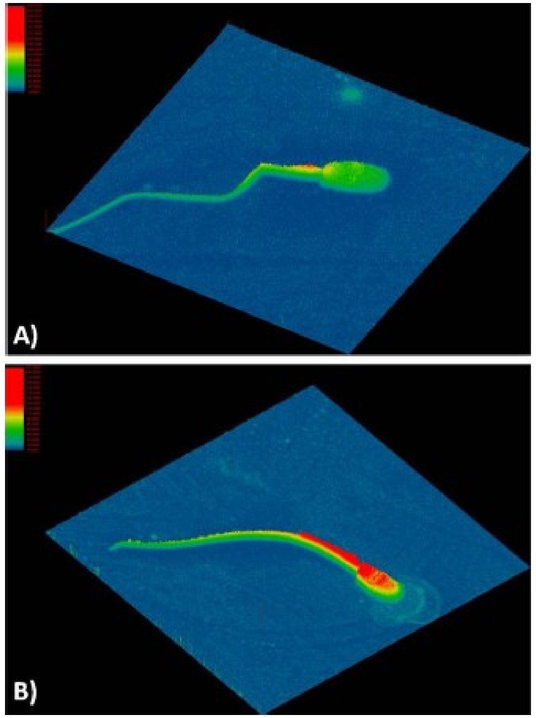

Figure 3 Confocal image representing actin localization in ejaculated and in capacitated spermatozoa. Confocal image representative of TRITC-phalloidin distribution on freshly ejaculated spermatozoon showing a faint fluorescence emission over the midpiece and post-acrosomal region (pattern A; panel A) and of incubated spermatozoon, displaying high fluorescence emission over the whole head (pattern B; panel B).

CTC

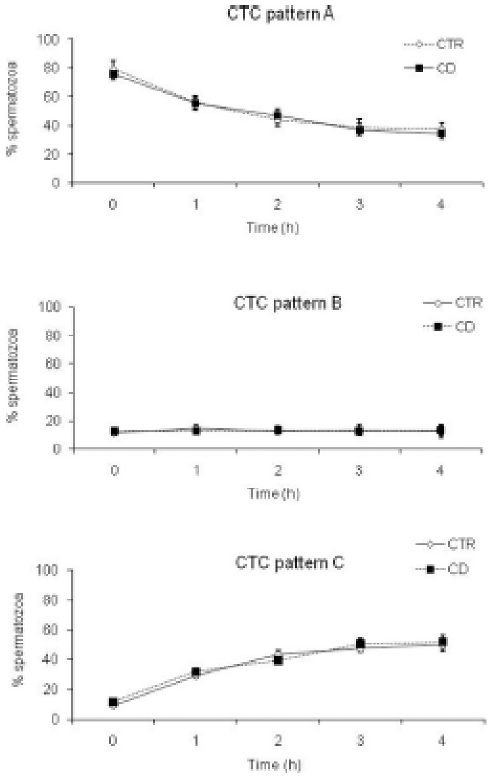

Figure 5 Kinetic of acquisition of CTC staining pattern A, B and C in CTR and CD treated spermatozoa. Graphic showing the percentage of spermatozoa displaying the CTC pattern A, B and C, during the 4 h of incubation under control conditions (dark continue line) or in the presence of CD (dark dot line). All the values are represented as mean ± SD.

protein tyrosine phosphorylation

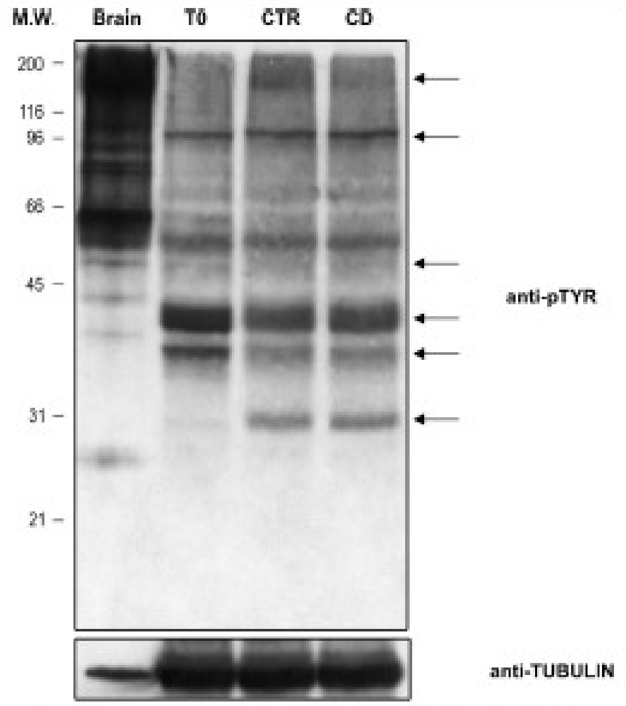

Figure 6 Tyrosine phosphorolation pattern in ejaculated and in capacitated spermatozoa Western Blot analysis of tyrosine phosphorylation pattern in total lysate of freshly ejaculated male gametes (T0) or in spermatozoa incubated under control condition (CTR) or in the presence of CD (CD). The arrows indicate the capacitation-related changes in P-Tyr. Brain proteins were used as positive control. The filter was normalized on the Tubulin expression. The data shown were representative of three independent experiments.

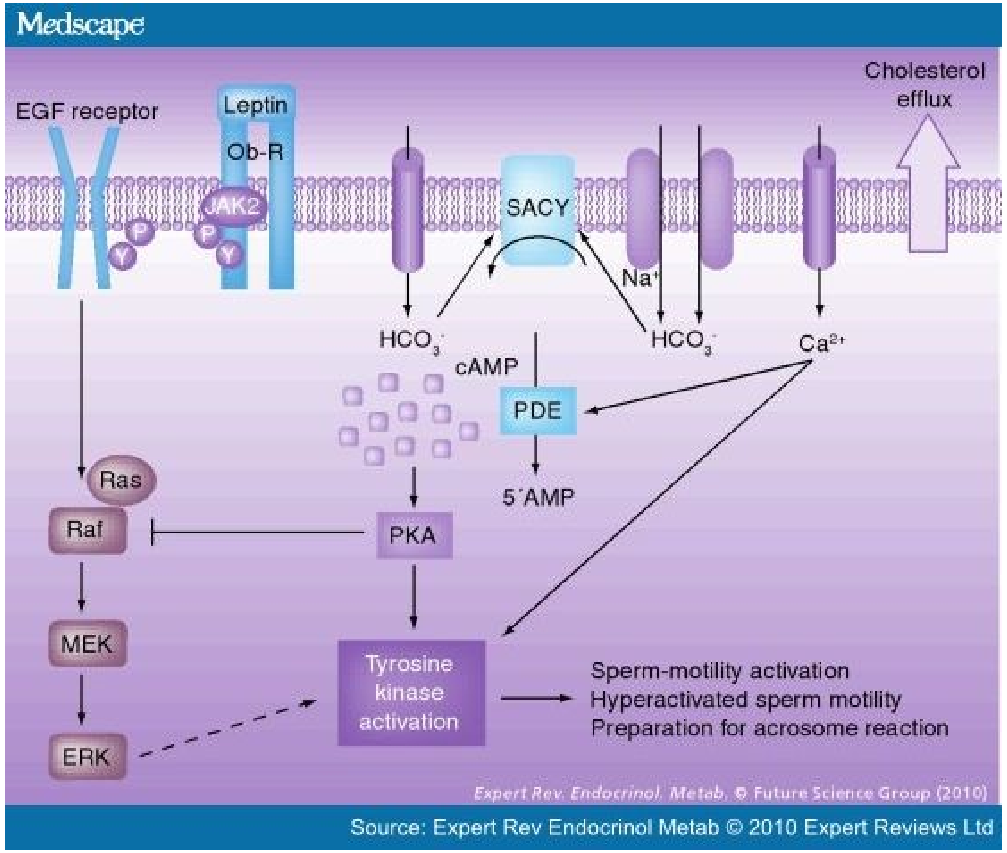

PLC-γ1

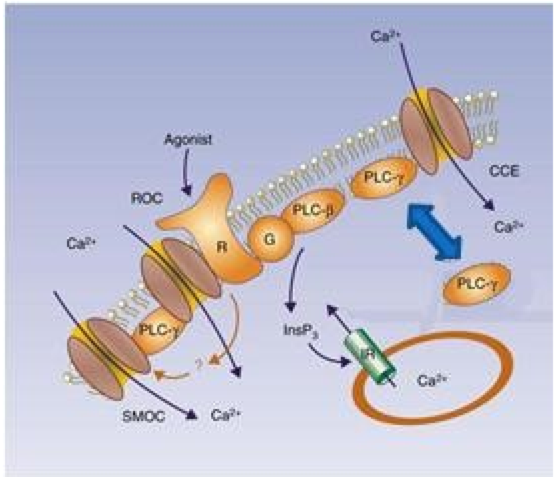

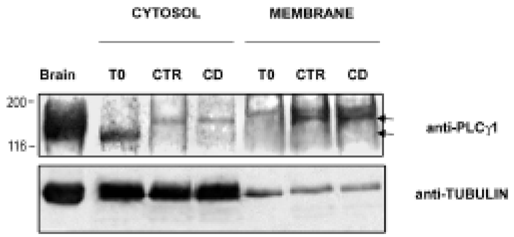

Figure 7 Capacitation-dependent PLCγ1 relocalization. Western Blot analysis of PLCγ1 localization in cytosolic and membrane fractions of freshly ejaculated male gametes (T0) or in spermatozoa incubated under control condition (CTR) or in the presence of CD (CD). The data showing the capacitation-dependent translocation of PLC-γ1 (arrows) from cytosol to membrane. Brain proteins were used as positive control. The filter was normalized on Tubulin expression. The data shown were representative of four independent experiments.

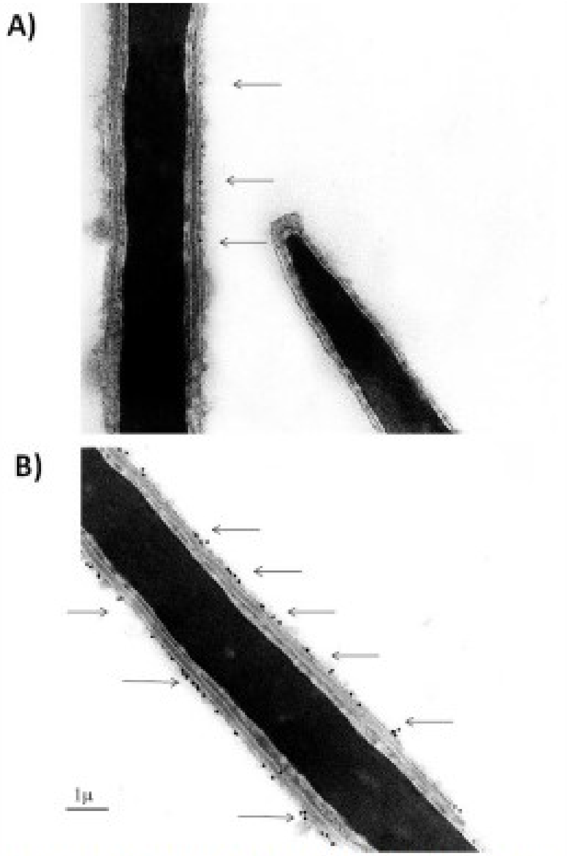

Figure 8 Transmission electron microscopy pictures demonstrating the topography of capacitation-dependent PLCγ1 relocalization. Transmission electron microscopy pictures (30.000X) showing: panel A): ejaculated spermatozoon displaying few gold particles (arrows) indicative of a low localization of PLCγ1 protein over cell membranes. panel B): in vitro capacitated spermatozoon incubated in the presence of CD that localized on its membrane several gold particles (arrows).

Ca^{2+}

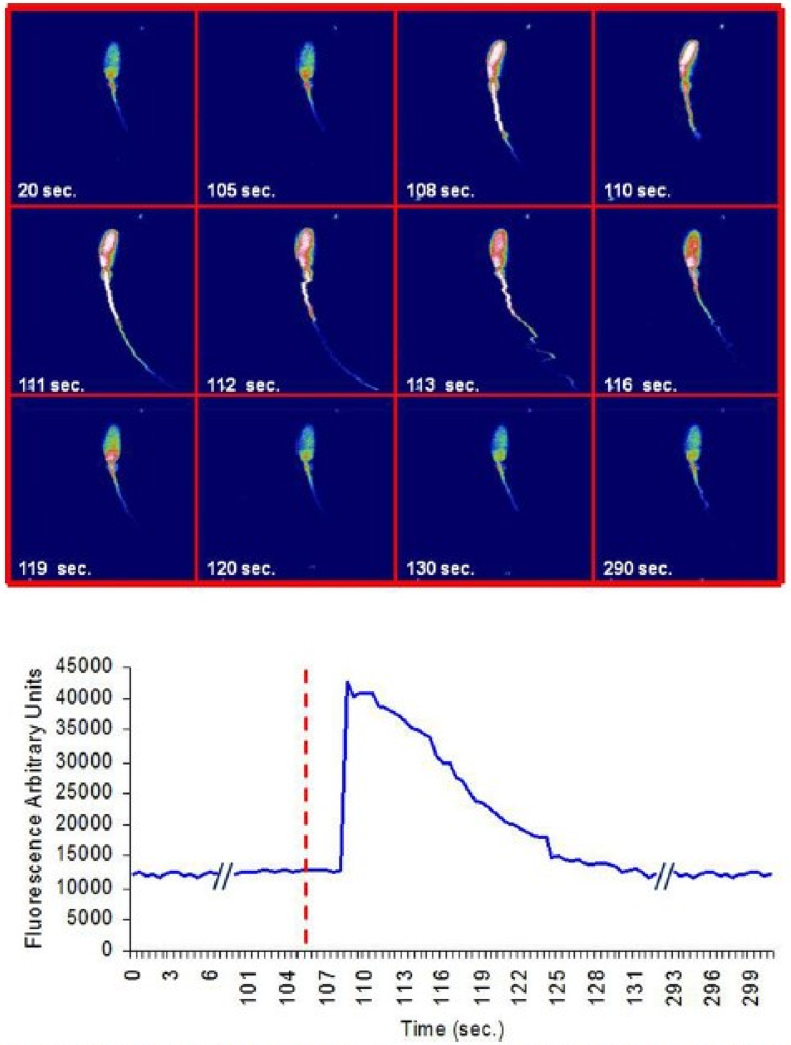

Figure 9 An example of confocal image gallery of CD treated spermatozoa loaded with Fluo-3AM exposed to sZP. An example of confocal image gallery of CD treated spermatozoa loaded with Fluo-3AM exposed to sZP (vertical red line). Notice that the rise in the $[Ca^{2+}]_i$ in spermatozoon is evident after <10 sec. from sZP addition, whereas return on the baseline occurs after about 30 sec.

Acrosome reaction

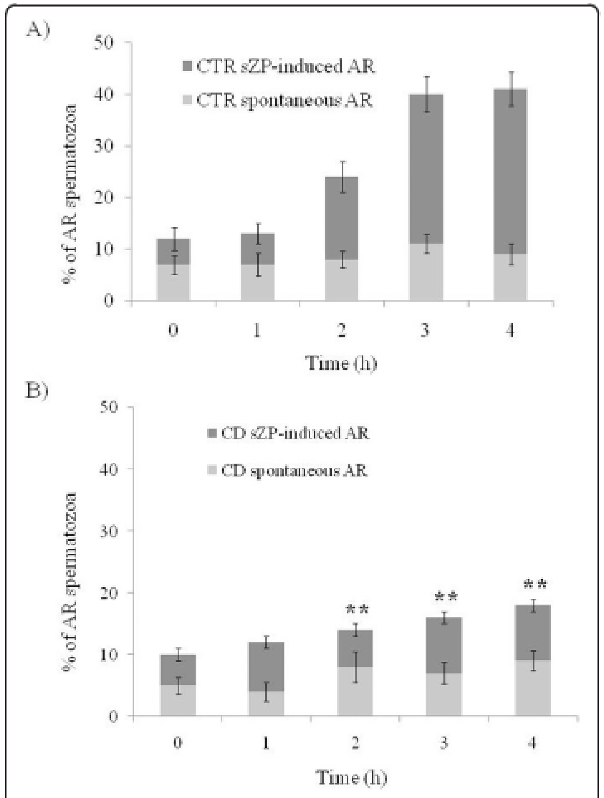

Figure 4 Histogram representing the percentage of spermatozoa undergoing spontaneous and sZP-induced AR in CTR (A) and CD (B) treated spermatozoa. Histograms showing the percentage of spermatozoa undergoing spontaneous (light gray) or sZP-induced (dark gray) AR in spermatozoa incubated under control conditions (panel A) or in the presence of CD (panel B). All the values are represented as mean ± SD. ** = p < 0.01 vs. CTR.

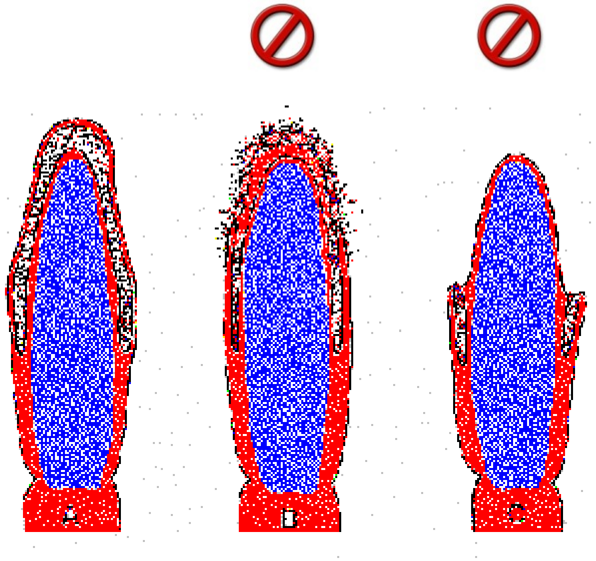

In conclusion

- The model has been validated;
- A new role of actin during sperm capacitation has been proposed.

Evolution of the system

Bioengineering & Biomedical Science

Bernabò et al., J Bioengineer & Biomedical Sci 2012, S3
http://dx.doi.org/10.4172/2155-9538.S3-001

Research Article Open Access

Signaling Strategy in Spermatozoa Activation of Sea Urchin, *C. elegans* and Human: Three Different Players for the Same Melody

Nicola Bernabò*, Ilaria Saponaro, Mauro Mattioli and Barbara Barboni

Department of Comparative Biomedical Sciences, University of Teramo, Teramo, Italy

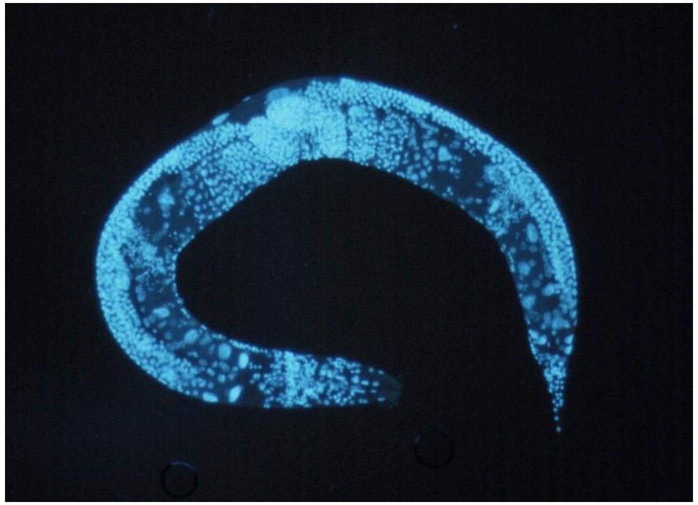

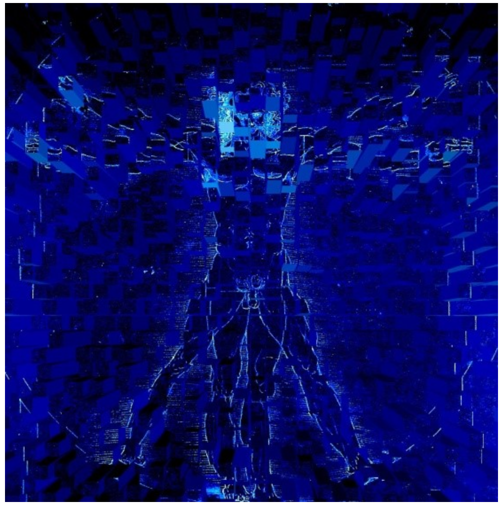

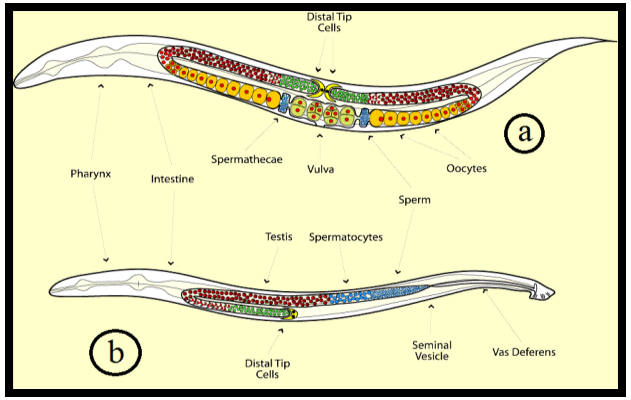
Distal Tip Cells
a
Pharynx
Intestine
Spermathecae
Vulva
Oocytes
Sperm
Testis
Spermatocytes
b
Distal Tip Cells
Seminal Vesicle
Vas Deferens

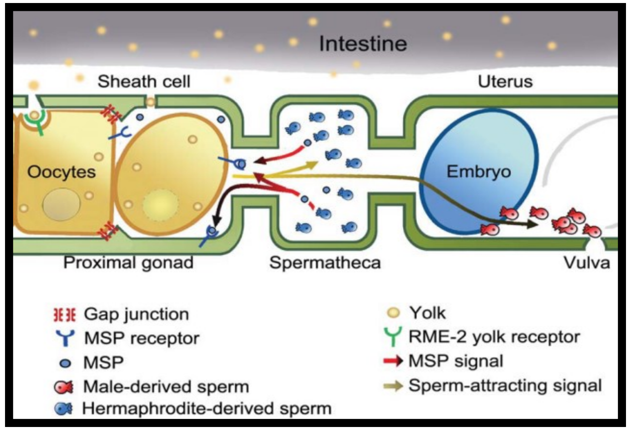
Intestine
Sheath cell
Uterus
Oocytes
Embryo
Proximal gonad
Spermatheca
Vulva
Gap junction
MSP receptor
MSP
Male-derived sperm
Hermaphrodite-derived sperm
Yolk
RME-2 yolk receptor
MSP signal
Sperm-attracting signal

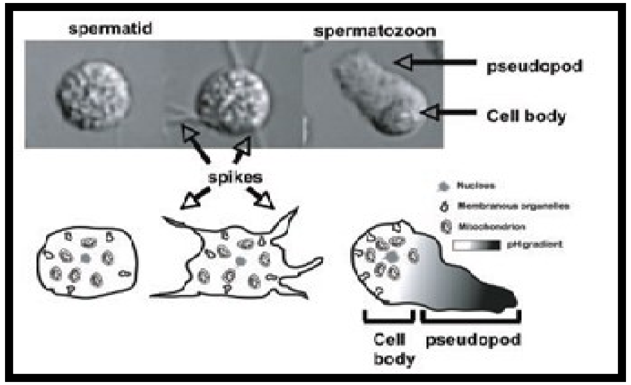
spermatid
spermatozoon
pseudopod
Cell body
spikes
Cell body
pseudopod

	Sea urchin	***C. elegans***	**Human**
Symmetry	Fivefold	Bilateral	Bilateral
Sexes	Male/Female	Hermaphrodite/ Male	Male/Female
Fertilization	External	Internal	Internal
Sperm motility	Flagellum	Amoeboid	Flagellum
Acrosome reaction	Yes	No	Yes
Membrane remodeling	No	Yes	Yes
Cytoskeleton remodeling	Actin	MSP	Actin
Time for sperm activation	Seconds	Days	Hours to days

Table 5: Main biological characteristics of reproduction and spermatozoa in sea urchin, *C. elegans* and Human.

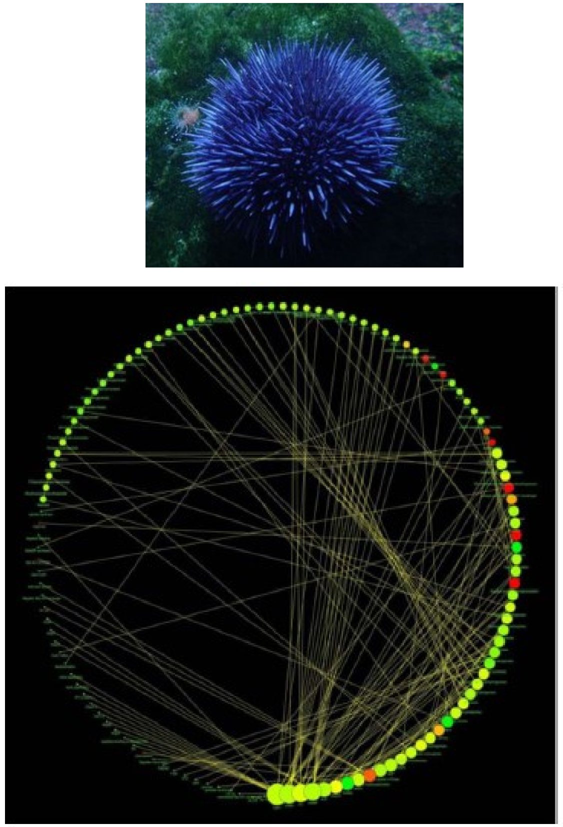

The nodes diameter is proportional to the number of links, the color varies depending on the closeness centrality (see text for explanation). The networks were spatially represented using the Cytoscape Degree Sorted Circle Layout: all nodes woth the same number of links are located together around the circle (see Cytoscape's User Manual).

Figure 1: Diagram showing the sea urchin spermatozoa activation network.

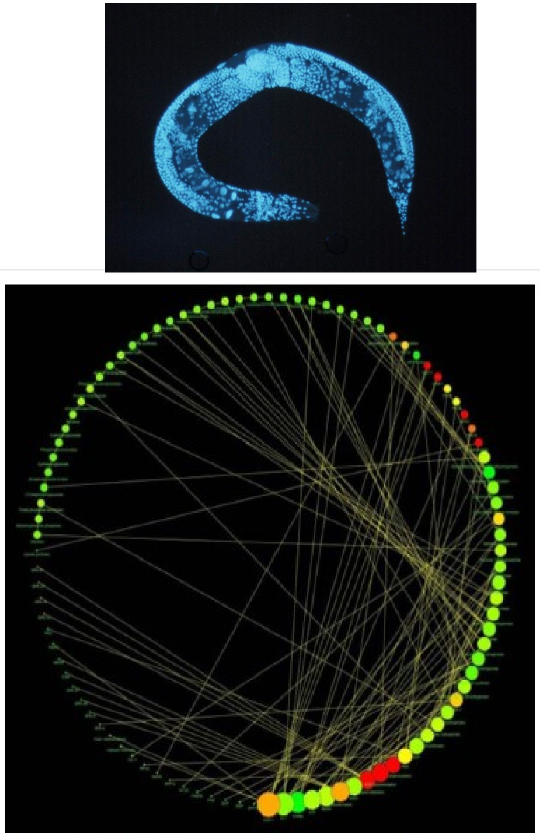

The nodes diameter is proportional to the number of links, the color varies depending on the closeness centrality (see text for explanation). The networks were spatially represented using the Cytoscape Degree Sorted Circle Layout: all nodes with the same number of links are located together around the circle (see Cytoscape User Manual).

Figure 2: Diagram showing the *C. elegans* spermatozoa activation network.

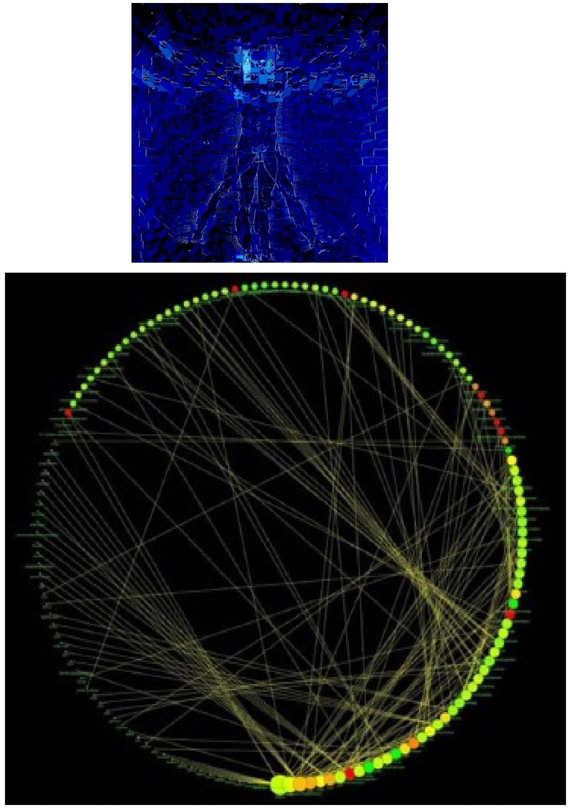

The nodes diameter is proportional to the number of links, the color varies depending on the closeness centrality (see text for explanation). The networks were spatially represented using the Cytoscape Degree Sorted Circle Layout: all nodes with the same number of links are located together around the circle (see Cytoscape User Manual).

Figure 3: Diagram showing the Human spermatozoa activation network.

	Sea urchin	*C. elegans*	Human
N° nodes	127	100	151
N° edges	175	132	202
Clustering coefficient	0.023	0.032	0.028
Diameter	23	23	20
Avg. n° neighbours	2.740	2.620	2.662
Char. path length	8.128	7.816	6.546

The number of nodes represent the total number of molecules involved; the number of edges represents the total number of interactions; the clustering coefficient is calculated as $CI=2nI/k(k-1)$, where nI is the number of links connecting the kI neighbours of node I to each other; the network diameter is the largest distance between two nodes; the Averaged n° neighbours represents the mean number of connections of each node; the Char. path length gives the expected distance between two connected nodes.

Table 1: Main topological parameters of Sea urchin, *C. elegans* and Human spermatozoa activation networks.

	Sea urchin		*C. elegans*		Human	
	IN	**OUT**	**IN**	**OUT**	**IN**	**OUT**
R	0.998	0.967	0.992	0.971	0.988	0.997
R^2	0.748	0.924	0.866	0.884	0.890	0.828
b	-1.589	-2.421	-2.067	-2.127	-1.542	-1.993

Table 2: Results of power law fitting of IN and OUT sea urchin, *C. elegans* and Human spermatozoa activation networks.

Sea urchin		*C. elegans*		Human	
Node	**N° of links**	**Node**	**N° of links**	**Node**	**N° of links**
$[Ca^{2+}]_i$	19	**$[Ca^{2+}]_i$**	10	**$[Ca^{2+}]^i$**	25
$[H^+]_i$	14	**$[H^+]_i$**	9	**Tyr phosph.**	13
ATP	9	**ATP**	7	**ATP**	15
cGMP	15	**Motility**	8	**PKA**	9
cAMP	13	**Vesicle fusion**	7		
		NADH	7		
		NAD^+	6		
		Pseudopod extension	6		

Table 3: Most connected nodes (the hubs) of sea urchin, *C. elegans* and Human spermatozoa activation networks.

In conclusion

- Different organisms share the same topology

Possible applications

- Contraception;
- unexplained infertility;
- Personalized medicine;
- in vivo – in vitro - in silico systems

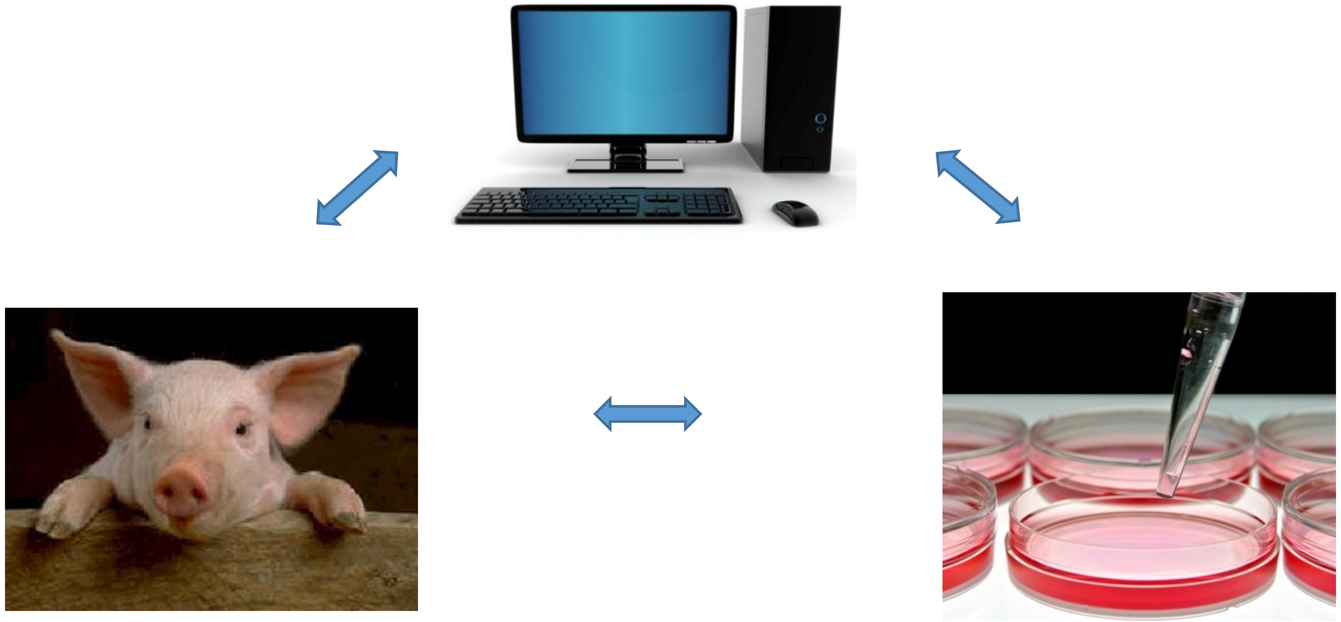

Human Sperm Interactome

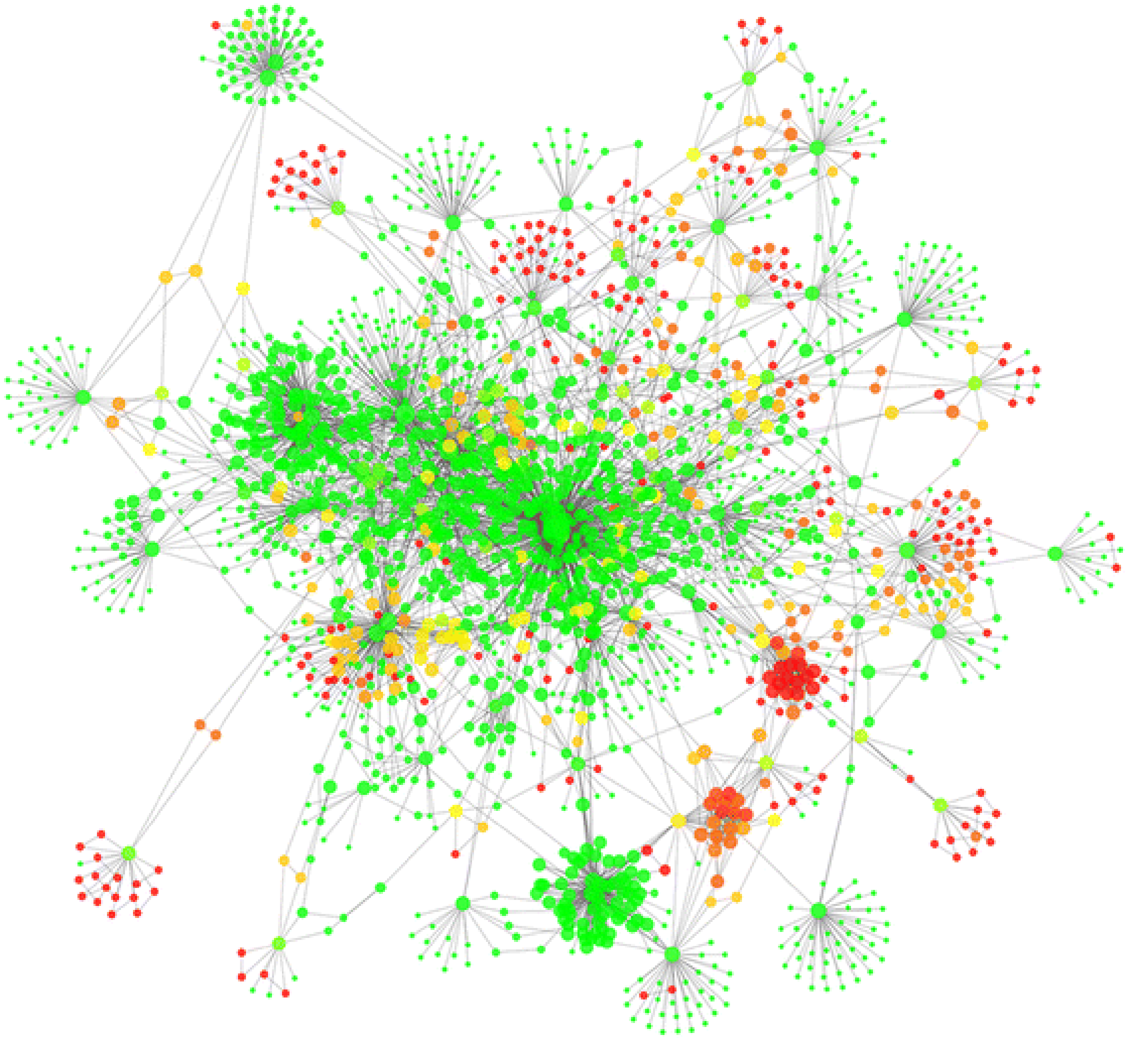

Thank You!